POLITECNICO DI TORINO

Department of Mechanical and Aerospace Engineering

MSc Thesis
in Biomedical engineering

Human Body Model and Passive Safety of Vehicles: Analysis of biomechanical results and study of injuries on abdomen organs

Tutor
Prof. Eng. Alessandro Scattina
Co-tutor
Prof. Eng. Christophe Bastien

Candidate
Giulia Vicini

October 2021

Index

Abstract

Every day people have a car accident and safety in the car becomes more and more an important requirement. Crash safety tests are still used today to understand how safe the vehicle is for the occupants, and which improvements can be made. Furthermore, they are very expensive and limited in predict injuries, so companies have begun to aim for another approach, the Finite Element Method (FE).

Total Human Model for Safety (THUMS) was introduced in computer analysis of vehicle collision. It is a human body computational model, which allows simulating the behaviour of the human body during impacts, giving a more accurate injuries prediction than rigid dummies tests.

THUMS is still an imperfect instrument, the aim of this thesis is trying to make changes to render the model more realistic, basing on human body properties. It is then validated comparing it to cadavers' behaviour for different types of impacts.

THUMS investigation presented in this study has focused on thoracic and abdomen organs, especially costal cartilage, thoracic fat, clavicles, liver, and spleen. Material's changes, based on literature, were preferred than geometric aspects to improve the model. A better definition of costal cartilage and clavicles is proposed, an analysis of thoracic fat's properties is conducted, and the liver and spleen's materials are completely modified. THUMS is validated after each change. In the validation phase, biomechanical results are analyzed and compared with corridors obtained with cadaver tests to understand if the modifications influence the THUMS' behaviour.

Preface

THESIS INTRODUCTION

This thesis work, made in collaboration with Professor Bastien of Coventry university and Giulia Mondino of Politecnico of Torino, originated to improve the PVP method, an innovative injury criterion. This energy-based criterion can be used to calculate the injuries severity of internal organs, which will be compared to the real one.

This is possible by modelling car crashes using the Total Human Model for Safety (THUMS), a human body computational model which allows simulating the behaviour of the human body during impacts. The more the model is accurate, the more the simulation's results will be similar to reality.

This thesis aims to analyze organs' properties to check their bio-fidelity. Thorax is one of the most involved parts during impacts; for this reason, this study focused on this area. Thoracic organs are taken into account and once the changes are introduced to better imitate the real ones, the new THUMS obtained is tested again. This is what is called the THUMS validation process, used to control the accuracy of the model responses. It consists of simulations of those which are considered the most dangerous impacts that happen during car crashes. The validation models use THUMS and simple components, which should represent internal car components, with the purpose to obtain those loads that impact the body during crashes. Using this process, the THUMS' responses are then compared to the corridors, which are the answers obtained by cadavers tested in the same conditions. These corridors create also areas in which curves must fall to ensure that model could be considered a good imitation of the human body.

The first chapter of this thesis is an introduction to the THUMS model, describing its features and its role in computer analysis. Next, in the second chapter there will be explained what the validation process is and its purpose.

In the third chapter, a state of the art of all human organs considered in this study is presented.

In chapter 4 the PVP method is briefly explained to better describe the origin of the thesis work.

The real core of this study is described in chapters fifth and sixth. Validation of the THUMS is shown in chapter 5, and since some curves do not reflect human behaviour, THUMS changes, discussed in chapter 6, are attempted to fix the model and make it more realistic than previous. A better definition of costal cartilage is proposed, an analysis of thoracic fat's properties is conducted, and clavicular cortical bone is better defined. Finally, liver and spleen's materials are completely modified to better imitate their real behaviour, since these organs are considered in the PVP analysis.

Chapter 1

HUMAN BODY MODELS (HBMS)

Cars have become an essential element in everyday life and for this reason, it is important to be safe while driving. Hence, the crash safety test has become increasingly important to give a measure of the vehicles' reliability.

At first human cadavers or animal, corpses were exploited for car crash tests, but with the introduction of rigid dummies, ethical problems were overcome [1]. Moreover, they allow having a biomechanical answer of the human body during the impacts, predicting its injuries severity. For this purpose, there are dummies for different types of impact, for example, the frontal one, the rear or the side.

Despite all, they are expensive and limited in predict injuries, so companies have begun to aim for another approach basing on the Finite Element Method (FEM): the Human Body Models (HBMs). They are computational models, based on human's body geometry and anthropomorphic material, which simulate the behaviour of the human body during an impact. A large amount of population is represented with HBMs, male, female or children, giving a more accurate injuries prediction than tests on rigid dummies. Nevertheless, HBMs are not frequently used in the industry, since they lack posture variety. They are, therefore, a modern tool which has to be improved.

Nowadays, there are several whole-body human models, like H-model, THUMS, and GHBMC. THUMS will be used in this thesis, the original Academic Version 4.02 AM50 Occupant model.

1.1 Total Human Model for Safety

THUMS (Total Human Model for Safety) is a human body finite element model developed by Toyota Motor Corporation and Toyota Central R&D Labs., Inc. It is a virtual model able to imitate human body behaviour during car accidents [2], which allows to better understand any injury.

THUMS includes not only the bones but also internal organs and muscles. It is also modelled on different genders (male or female) and ages to reproduce the greatest range of people (Figure 1). The purpose on which THUMS is based is to give a robust tool for safety testing of car crashes. For this reason, Toyota engineers work to improve more and more the models of the different parts of the human body, refining meshes and material properties.

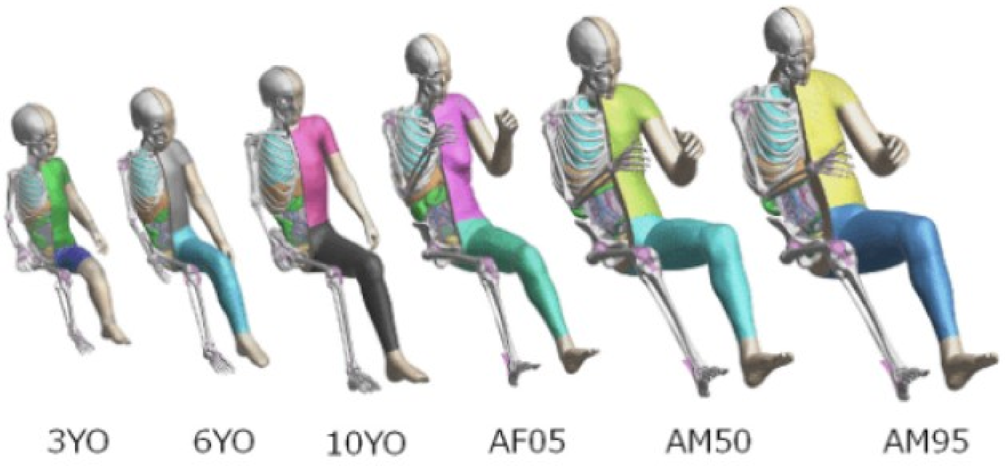

Figure 1 - *THUMS occupant models for different ages and different percentile [2]*

In this thesis, an Academic Version 4.02 AM50 Occupant model is used, built to fit the 50th percentile of the American male.

Version 4 adds, concerning previous versions, a more detailed model for internal organs since they are one of the most fragile parts during impacts (Figure 2).

The occupant is a THUMS modelled on a person who is sitting in a car, so it is different by the pedestrian-only for the posture, indeed, the pedestrian has a standing posture.

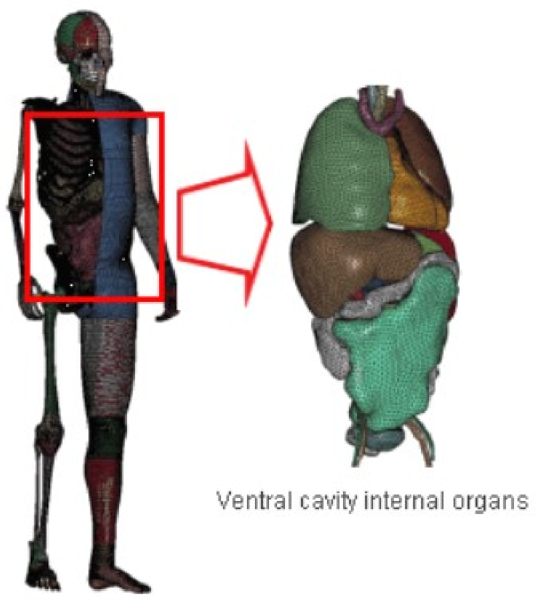

Figure 2 - *THUMS version 4 [2]*

Chapter 2

TORSO OCCUPANT VALIDATION

In Japan, Zhao et al [3] advanced research about which type of crashes are often and which parts of the body are involved. According to this study, frontal and lateral crashes are very common, so the head, the thorax, and the abdomen are the parts of the body at the highest risk. Even belted and unbelted occupants were observed and, as result, it was noticed that belted occupants suffered less serious injuries.

To understand if a new version of the THUMS can predict injuries and biomechanical response, the first step is the validation, which means simulating those impacts that turned out to be dangerous. The purpose is to achieve a model that better reflects real human tissues properties obtaining a behaviour similar to the human body during impacts. This is the best way to get accurate information about automotive safety.

Hence, every time an impact is simulated, curves must be extracted (usually force-time, deflection-time, and force-deflection) to establish the bio fidelity of the model. It consists in comparing the curves with corridors, data obtained from the same impact realized in vivo with Post mortem Human Subject (PMHS). If the curves fall into the range defined by the corridors, the model can be considered validated.

This topic is considered very interesting, and, for this reason, it is investigated by different scientists. They tried, indeed, to recreate simple elements, which should represent internal car components, with the purpose to obtain those loads that impact the body during crashes.

2.1 Thorax validation

Three types of impacts belong to this category. The thorax is tested in the frontal and lateral sides and with the seat belt.

2.1.1 Frontal impact

The first type of validation presented in this thesis is Frontal impact validation. As mentioned before, Kroell et al [4, 5] wanted to recreate the load in which the steering wheel impacts against the thorax during a frontal car crash. 19-81 years old PMHS is used, 53-82kg in weight and 168-183 high.

As figure 3 shows, the seated and stationary cadaver was positioned with arms stretched forward in the steering wheel holding position. Depending on the case, you can use a different impactor and set different loading conditions. In this thesis, an impactor of 152 mm in diameter is used. It collides with the sternum between the 4th and 5th ribs with an impact velocity of 7.2 m/s for an impactor of 23.1 kg.

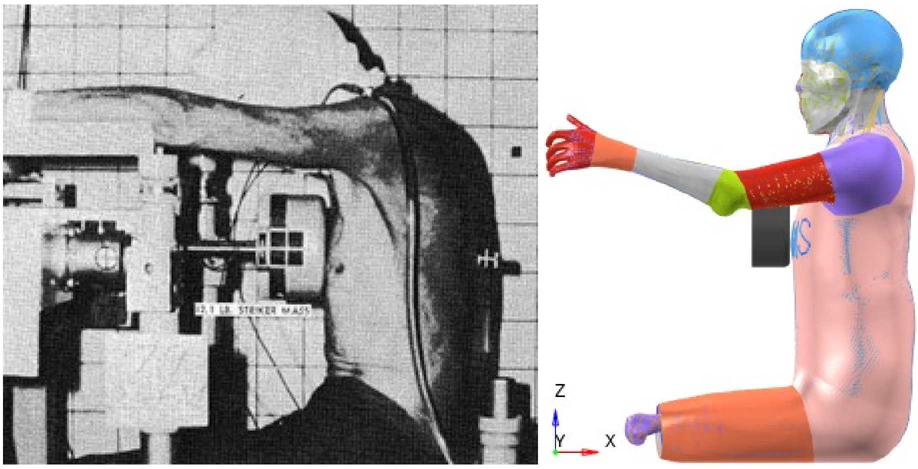

Figure 3 *- PMHS and THUMS Ver.4.02 AM50 for Thorax impact validation [4]*

When the impact occurs, the body moves and, in consequence, rotates and finally, the body could fall supine. This last movement only happens when the load no longer acts, for this reason, this circumstance does not need to be analyzed and no support for the back is requested.

To measure force and deflection (especially in the x-direction), the scientist used respectively accelerometers and high-speed photographic (1000-2000 pictures/s) looking for in the images the moment in which the impactor encountered the chest.

Through a different test setting, the frontal impact corridors were developed. In figure 4, it is shown an example of corridors, force versus deflection cross-plot.

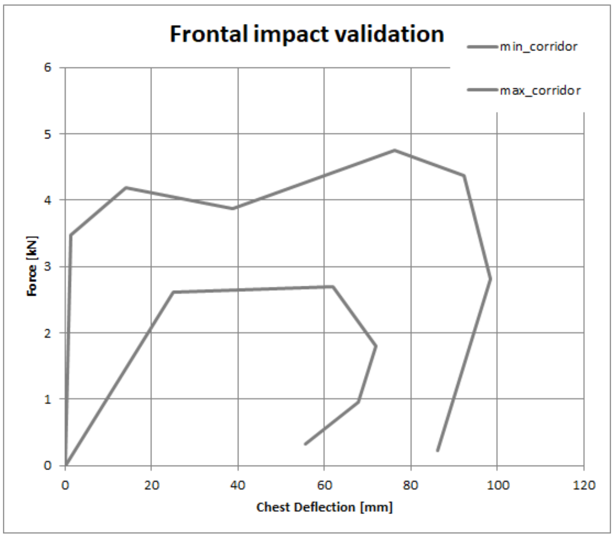

Figure 4 *- Corridors for Thorax impact validation*

2.1.2 Belt impact

With the introduction and use of the belt restraint system, it was necessary a belt impact with the thorax. It is crucial not only to validate THUMS but also to understand the role of this system in the biomechanical response.

Cesari et al [6] occupied this topic using 13 cadavers and 20 dummies, in a special test apparatus. It consists of a table on which is positioned the supine PMHS and, to recreate the car system, the cadaver is surrounded with the belt strap. The belt is fixed under the table and controlled by a bar, able to move up and down thanks to the impactor (figure 5). The impactor, colliding with a plate connected to the pulling cable, pulls the bar and, as a consequence, the belt with the same velocity as the impact.

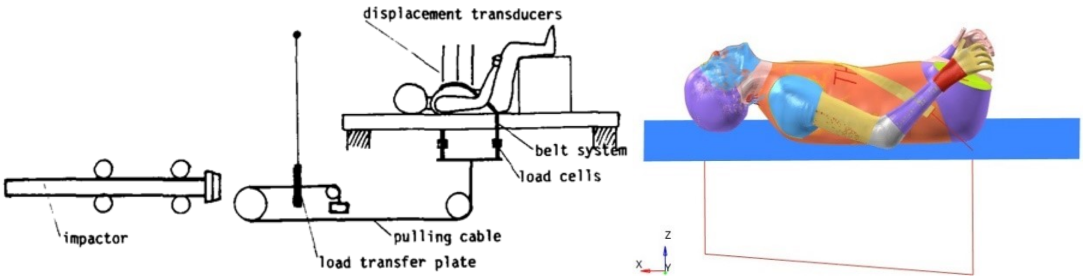

Figure 5 *- Representation and model of test apparatus [6]*

To understand the deflection of the thorax, scientists used displacement transducers in different points of the torso and three of them on the belt, the same points will be considered for THUMS validation (Figure 6).

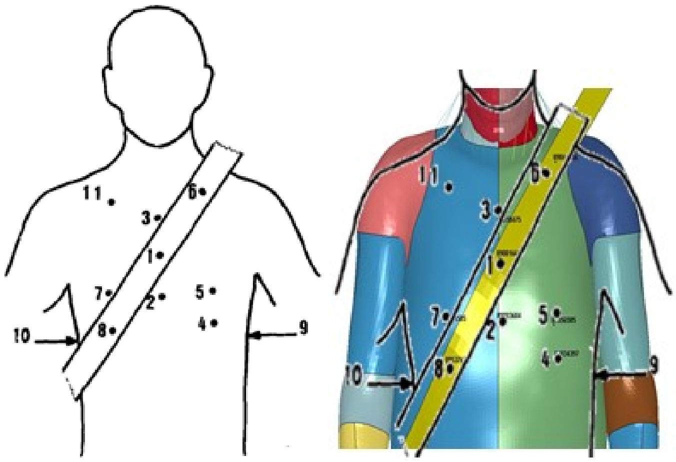

Figure 6 - On the left: Representation of nodes considered for deflection measures. On the right: THUMS version overlaid [6].

The ribs were analysed to understand if were not damaged and so appropriate to be subject to different tests, with both low and heavy mass for the impactor. Examining results, they discovered the right side suffered more than the opposite one, indeed a higher deflection for points 8 and 1 than all the other points.

Only the case that will be simulated in this thesis is considered for the validation of the THUMS: low mass impactor of 22.4kg and 7.78m/s of velocity impact. However, all results of all the tests were used to calculate the interval in which the maximum deflection must fall to validate models. (Figure 7).

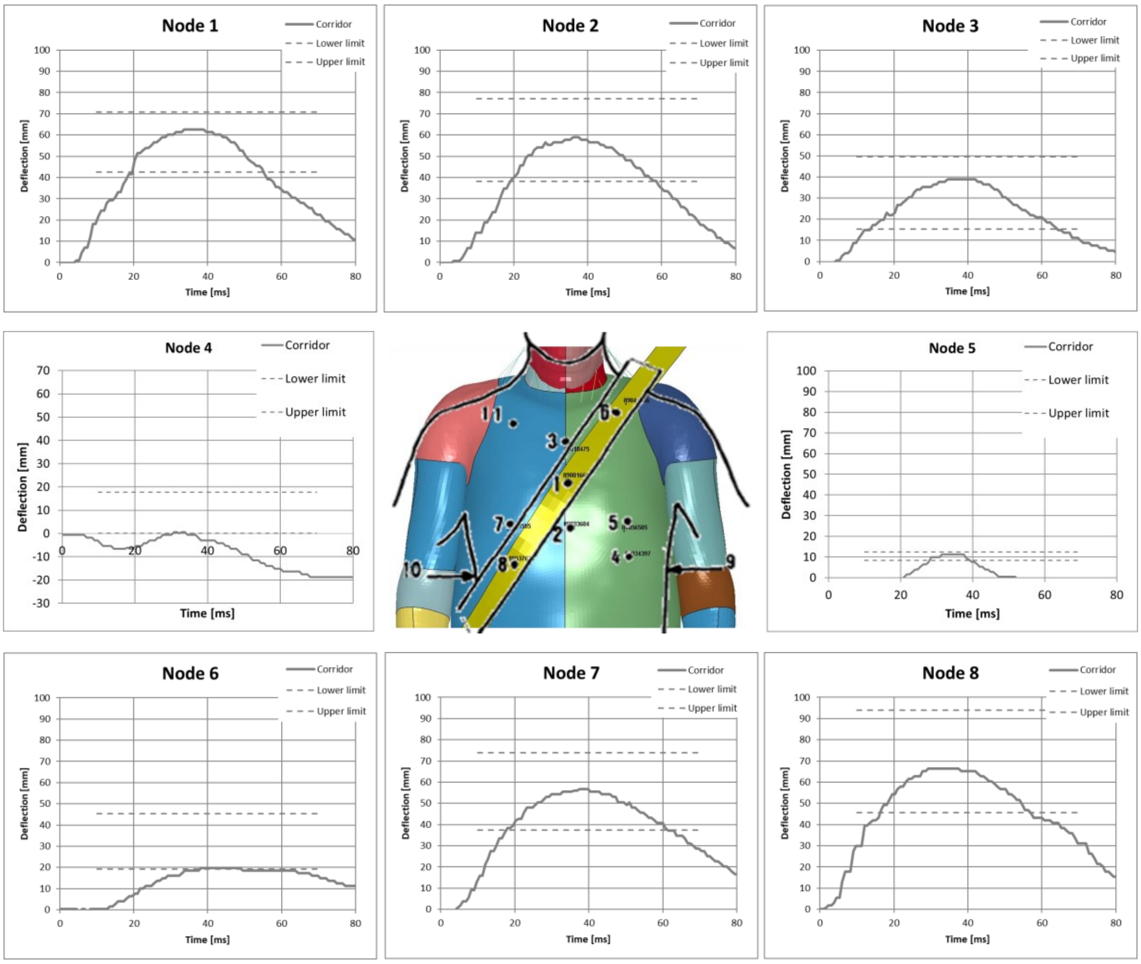

Figure 7 - Corridors for Belt impact validation: the Experimental curve is the corridor, and the deflection interval is represented with dotted lines

2.1.3 Lateral impact

Among the various causes of car accidents, one of the most frequent is the lateral impact, for this reason, this is simulated to validate models.

The original experiment was performed by Shaw et al. [7] with PMHS, whose purpose was to understand thorax behaviour in crashes considering different directions of impact. Hence, they used pendulum testing in seven subjects for lateral and oblique impact for each side of the body.

In this thesis, it is only considered the lateral impact. The pendulum test consists of an impactor which collides with the lateral side of the body, while THUMS has raised arms to make the impactor impact against the thorax. The impactor, of a diameter of 15.2 cm and 23.4 kg in weight, with a 2.76 m/s of impact velocity imposed, is positioned under the armpit. The PMHS is here tested on the right side, while in the model used for this thesis, the impactor is positioned on the left side of the THUMS which must be validated (Figure 8).

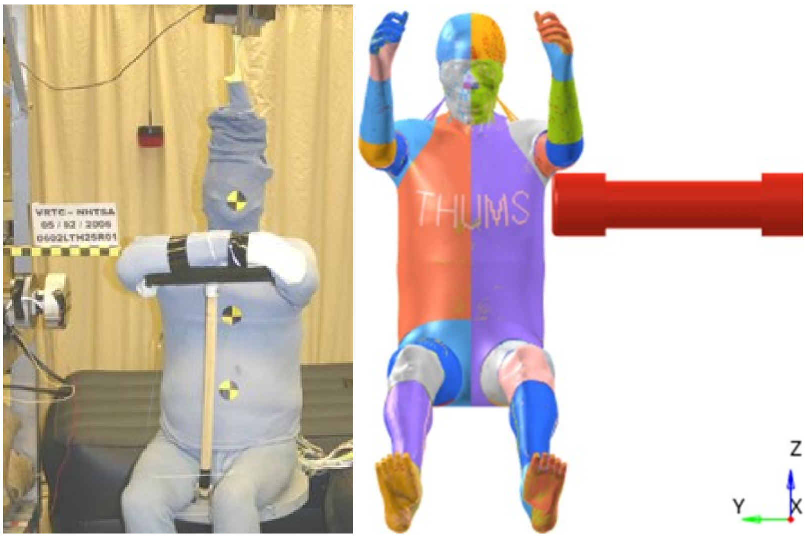

Figure 8 *- PMHS and THUMS Ver.4.02 AM50 for Lateral impact validation [7]*

As regards results, it is interesting to observe the impactor force versus the deflection of the thorax, of course in the y-direction.

In the experimental case, a chest band was used for deflection of the thorax, 40 accelerometers positioned across all the band. It is useful to obtain chest contours to understand in what directions the chest moves, indeed movements due to lateral impact evolve in more directions with respect to oblique impact (Figure 9), it is the reason why the later impact is the only one considered in the validation process.

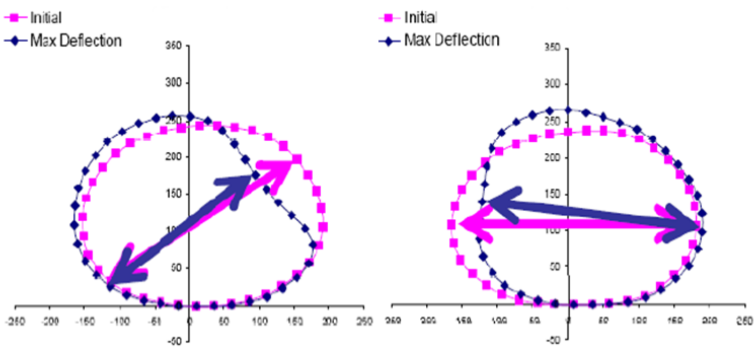

Figure 9 *- Oblique and Lateral Chest Band Contours [7]*

Then corridors are extracted from these experimental data to make them available for THUMS' curves comparison (Figure 10).

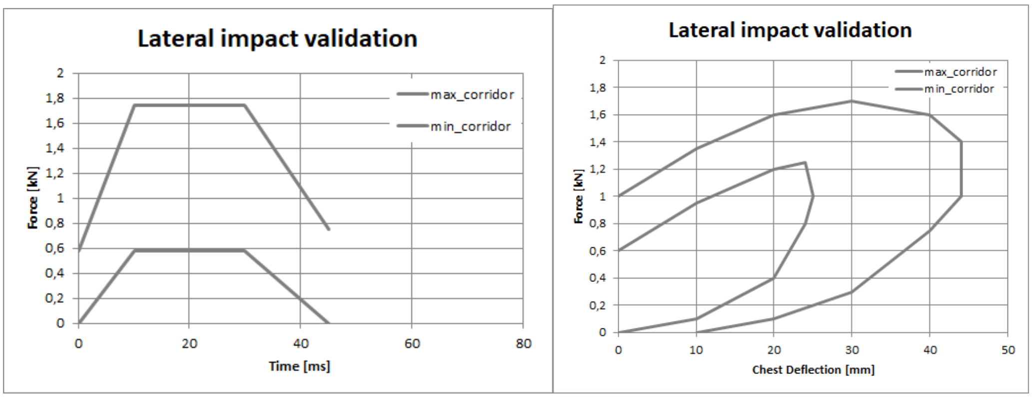

Figure 10 *- Corridors for Lateral impact validation*

2.2 Abdomen validation

After the thorax validation, another part of the body is subjected to injuries during crashes, the abdomen. It can be analyzed using both a bar and a belt-like impactor.

2.2.1 Bar impact

Firstly, the abdomen was analysed with a bar impacting the abdomen as explained in studies of Cavanaugh et al. [8] and displayed in figure 11. Cavanaugh et al utilized human cadavers to evaluate the abdominal human response and to investigate the behaviour of the liver, the kidney, and the spleen during a frontal impact (organs that were found to be more injured during the crash). For this purpose, they used 12 PMHS hit by an aluminium bar of 25 mm diameter, long 381 mm with a variable mass between 32kg-64kg. Different tests were processed, with different masses of impactors, for different velocities, from 4.9 to 13.1 m/s.

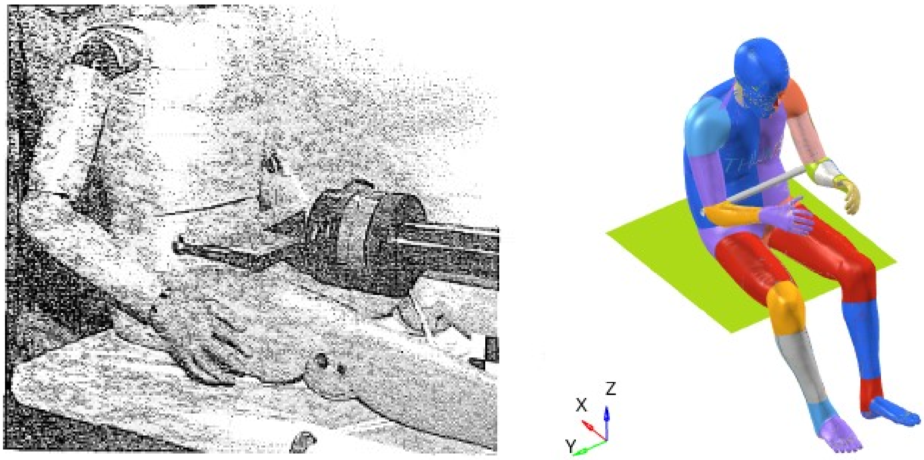

Figure 11 - Dummy and THUMS in abdomen impact [8]

In this way, the corridors were created, a cross plot between force and displacement for average lower and higher speed, respectively 6.1 m/s and 10.4 m/s (Figure 12).

To measure the force and the displacement, uniaxial accelerometers were placed in the impactor and, also, the abdominal impacts were filmed with a speed camera.

Other studies were performed on this validation test to recreate the corridors but, this thesis bases on Cavanaugh et al.'s study.

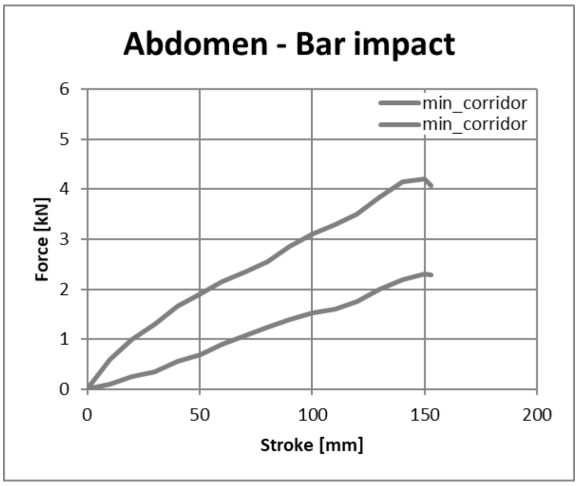

Figure 12 - Corridors for abdomen bar impact

2.2.2 Belt loading

After the study of bar impact, another analysis is conduct, in which the abdomen is stressed with a high-speed seatbelt.

The test, Hardy et al. [9], is conducted on cadavers, which are seated and loaded with a belt in the abdominal area with different speeds (from 3.0 m/s to 9.4 m/s). The output of the test is the displacements between the spine and seatbelt, measured by potentiometers.

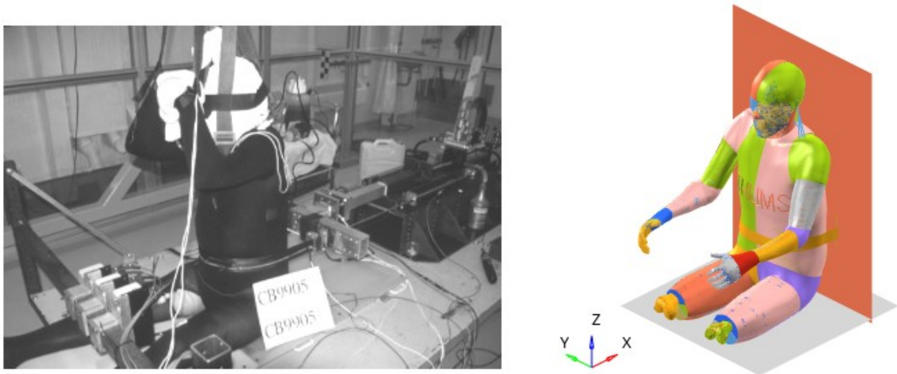

Figure 13 *- Typical test for abdomen impact with seatbelt [9]*

In this thesis, the validation test is based on Cavanaugh et al.'s [8] study, which recreates the same the Hardy et al tests. A correlation between the force, with which the seatbelt hit the abdomen, and displacement of the abdomen when it is stressed, is plotted in figure 14. Corridors are created using the two different tests in which different belt speeds were set.

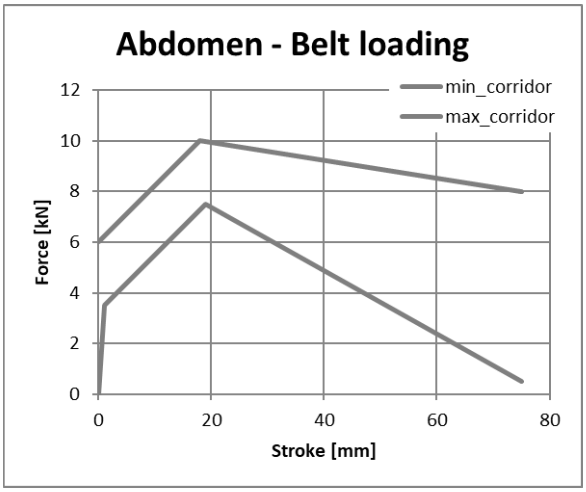

Figure 14 *- Corridors for abdomen impact with seatbelt*

2.3 Pelvis validation

According to studies on car accidents, the vulnerability of the pelvis was found. For this reason, the model has to be validated for the answer of the pelvis in impact.

2.3.1 Knee Thigh Hip impact

During a car accident, part of the car can often hit the knees. This force is passed on other parts of the body, as the thigh and hip. Some studies are made in order to understand as these parts of the body are loaded.

In Rupp et al. [10], a large number of tests are made. The knees are hit by a padded impactor, which has different velocities.

To recreate this test, in the validation phase the whole THUMS is used. The THUMS is seated, and the knees are hit by a table. The table is, also, put in motion with three different velocities.

After the simulation, the force at every instant of time is taken and then the comparison with the experimental data, given by Rupp et al's study, are made.

The figure 15 below shows the experiment and the corridors obtained in the Rupp et al.' article.

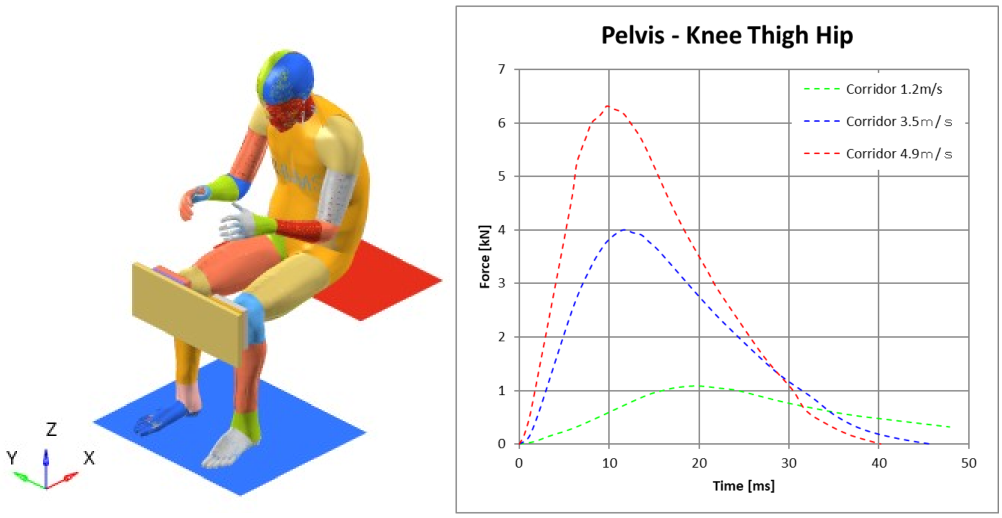

Figure 15 - Pelvis validation (Knee- Thigh -Hip): method [10] and corridors

2.3.2 Acetabulum lateral impact

Another test, basing on Guillemot et al. [11], is used to evaluate the problem of the pelvis. They analyzed different accidents, discovering the most common injuries in the pelvis. Then they made some dynamic tests to understand the behavior of the bones. For this reason, the pelvis was immobilized and put vertically. Then an impactor, with accelerometers, was brought down on the pelvis.

In the simulation, a simplified model is built to recreate the analysis, as reported in the figure 16. Finally, the validation is made with two different configurations for the parameters correlated to the fail of some materials. In this way, the inferior and superior corridors are created, and it is possible to make a comparison between the two limit cases.

In the figure 16 the recreation of the test, presented in the article, and the corridors are shown.

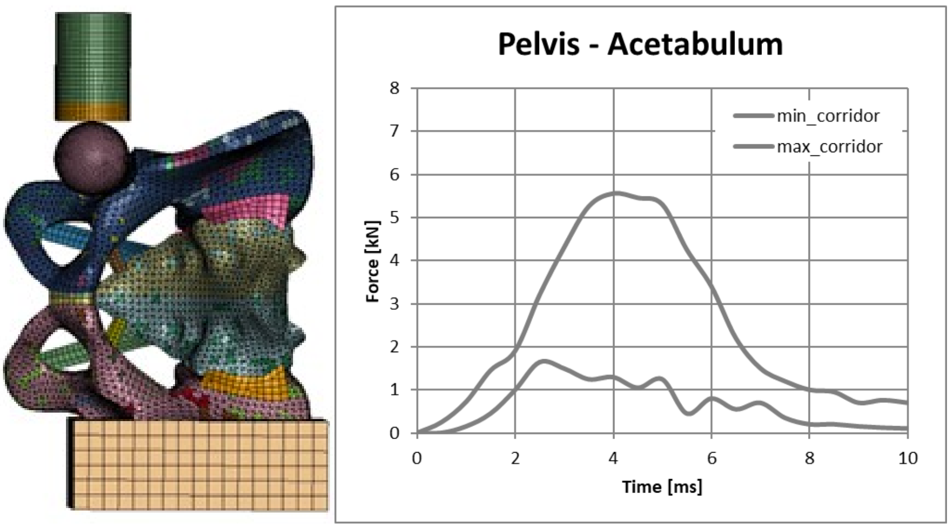

Figure 16 *- Pelvis (Acetabulum Lateral Impact): method [11] and corridors*

Chapter 3

ORGANS: anatomy and FE model

THUMS is modelled in order to imitate the human body. The position and properties, of the recreated organs, can have a great effect on the simulations. In this chapter, there will be presented every organ that, for several reasons explained in the next chapters, will be considered.

3.1 Thoracic organs

3.1.1 Costal cartilage

The ribcage is a very important part of the body because it protects all vital organs in the thorax. Costal cartilage just like 24 ribs, the sternum, and the thoracic vertebras belong to this. Thanks to the costal cartilage, ribs are articulated to the sternum from the first to the seventh; the eighth, ninth and tenth use the extension of the last costal cartilage. The eleventh and twelfth ribs are the floating ones because are not attached to the sternum but only to the thoracic vertebras (Figure 17) [12, 13].

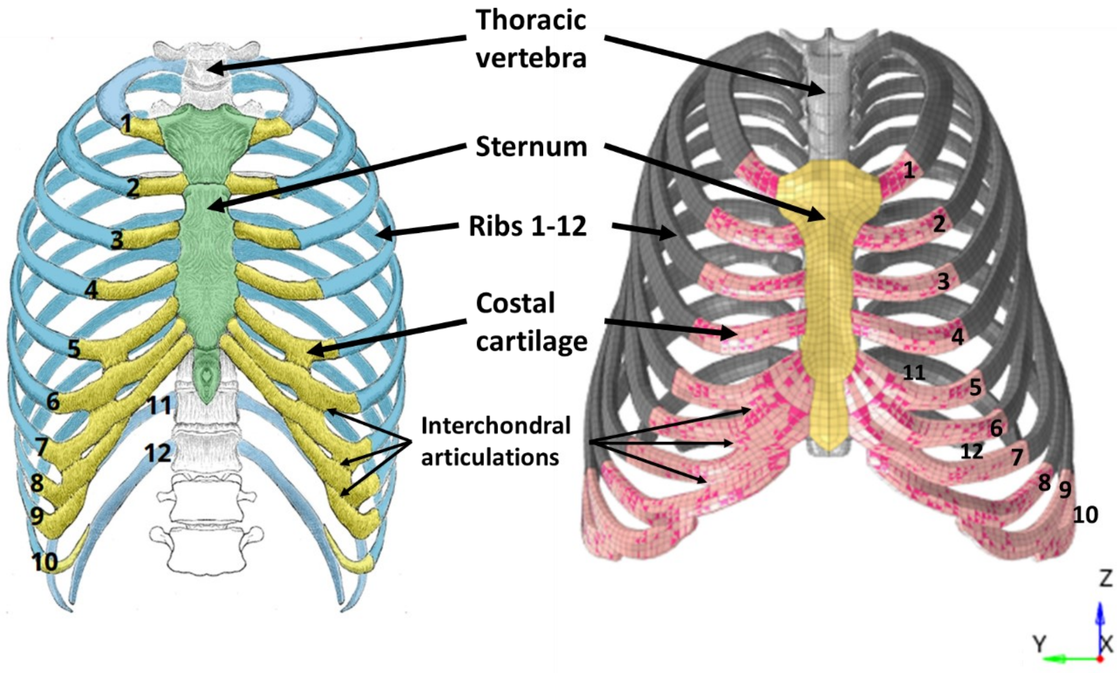

__Figure 17__ - Costal cartilage in human body [13] (left) and in the THUMS (right)

The costal cartilages change their geometrical form. The width is greater in the rib side than the sternum side, while the length increases until the seventh and then decreases again to the eleventh. Even their direction is not uniform passing from the first to the last costal cartilage.

The ribs-costal cartilage articulations, the inter-chondral articulations, are also showed in the figure. They connect costal cartilage from one to the other from the sixth to the tenth. They consist of an articular capsule, coated by a synovial membrane with some ligamentous reinforcing fibres. Anyway, the costal cartilage is not only connected to the ribs, but also to different thoracic muscles both in the interior and exterior side [12, 13].

FE model is quite similar to the real costal cartilage, but inter-chondral articulations are simplified in THUMS. Indeed, the borders are totally connected in the model, instead, the real ones are articulated only in some points.

The costal cartilage is composed of hyaline cartilage coated by the perichondrium, which is composed of oriented collagen fibers. Unlike the other parts of the ribcage, which are much more investigated, there is little research about this part. Moreover, they mostly focused on the cartilage substance alone and for this reason, costal cartilage is often modelled as a homogeneous material [14].

THUMS represents costal cartilage as a solid part, modelled with hexahedra elements, using the element formulation 1. In addition, a shell coating covers this part. The 16th formulation option is used for the mesh and, a null material is employed to better simulate the contact with the other parts of the chest.

A viscoplastic material, the number 105, the MAT_DAMAGE_2, which use continuum damage mechanics (CDM), is chosen to recreate costal cartilage. A stress-strain curve is defined by effective plastic strain values EPS and corresponding yield stress values ES.

3.1.2 Thoracic fat

Fat is adipose tissue, composed mainly of adipocytes. It is already considered as an endocrine organ producing hormones, and it is necessary for different tasks; the main ones are to store energy and cushion the human body [12, 13].

All adipose tissue located in the chest, between the pulmonary artery, around the hearth and the diaphragm, is called thoracic fat. It is composed of the epicardial fat and the pericardial fat, or the intrathoracic fat. The superficial fat of the hearth is the epicardial adipose tissue, mostly accumulated at the height of the valves. The pericardial adipose tissue which is above the visceral pericardium is functionally different from the epicardial fat, but clear boundaries are difficult to identify. Every organ needs alimentation, in this case, the coronary artery deals with epicardial fat sustenance, while the internal thoracic artery nourishes the pericardial one.

Adipose tissue can influence very hard the cardiac organ, with the bioactive molecules that it produces. It consists of almost 20% of the hearth weight, but probably the difficulties in its dissection could render these values not very accurate [15, 16, 17, 18, 19, 20, 21].

Figure 18 shows where thoracic fat is located in the human body's hearth and how it is presented in THUMS. Thoracic fat is simplified in THUMS, modelled as a unique solid component surrounding the hearth. This one is not the only difference; the element starts from far above the pulmonary artery and, its volume is not comparable with the real one. This last aspect will be discussed in chapter 6.

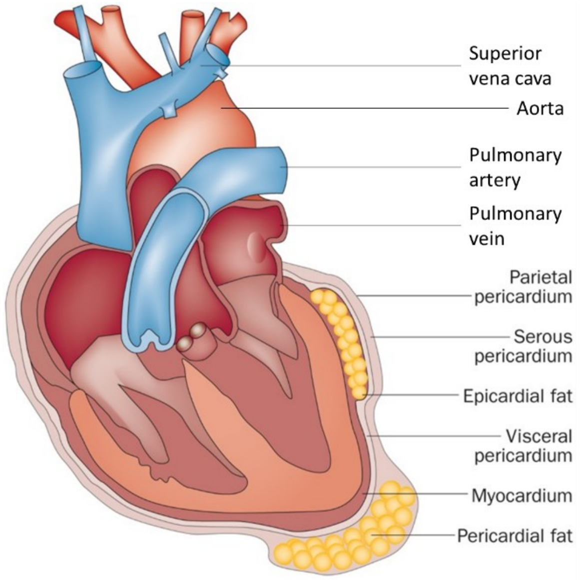

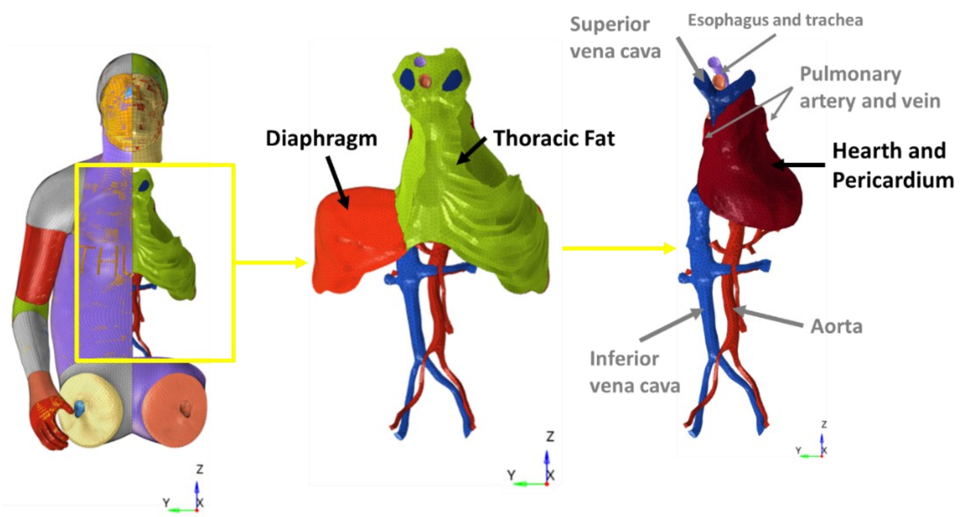

Figure 18 *- Thoracic fat in human body (above) and in the THUMS (below)*

The thoracic fat's mesh in THUMS is composed of tetrahedra elements, using the element formulation 13. It is modelled as a foam using material number 181, the MAT_SIMPLIFIED_RUBBER/FOAM, which is defined by a single uniaxial engineering stress-strain curve.

3.1.3 The Clavicle and its ligaments

The clavicle is one of the few palpable bones, a horizontal bone in the human body which role is to transfer forces to the skeleton from the arms, but most important to articulate the sternum to the shoulder blade (scapula) [12, 13].

These two bones connected give the name to the clavicle ends: the sternal end (or medial, SC joint) linked to the sternum through the sternoclavicular ligament, and the acromial end (or lateral, AC joint) linked to the acromion of the scapula through the acromioclavicular ligament. Both, the AC and SC are synovial joints, a fibrous capsule surrounded by fibrocartilage and with an intra-articular disc inside [22]. The clavicle is also related to the first rib thanks to the costoclavicular ligament and the coracoid of the scapula across the coracoclavicular ligaments. Finally, the shaft of the clavicle, the middle part, also is connected to different muscles like the deltoid, trapezius, subclavius, and sternocleidomastoid (Figure 19).

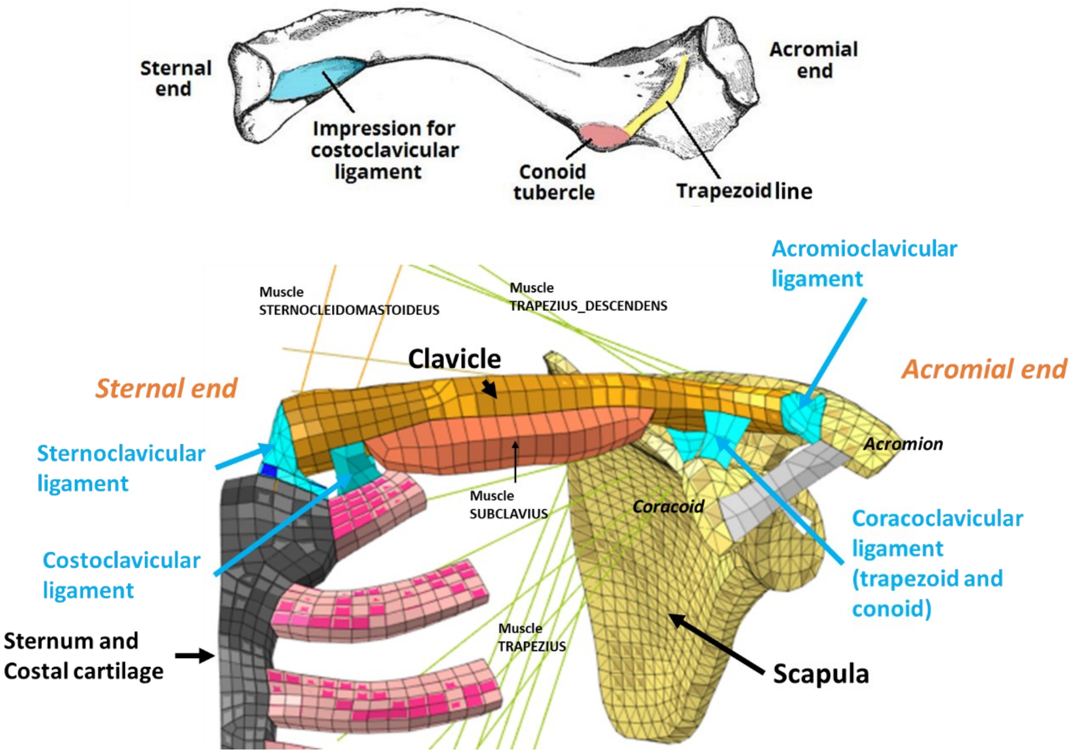

Figure 19 - Above: Representation of the clavicle in the human body [13]. Below: Clavicle representation in the THUMS

The clavicle is classified as a long bone for its shape, but it has the typical organization of flat bones: spongy bone covered by cortical bone thicker in the middle. This bone has a sigmoid curve, one curve is convex, and one is concave; there is also a medullary canal with a different size and shape along the bone [23].

It is one of the most fractured bones, especially during car crashes and 80% of fractures occur in the middle of the shaft, while only 15% in the lateral and 5% in the medial side. National Automotive Sampling System's Crashworthiness Data System (NASS-CDS) found that 90% of fractures during frontal impact happen in the clavicle because of the belt loading [24, 25, 26]. Less common is dislocation, the AC and SC joints can usually risk this type of injury during contact sports [22].

The clavicle model is similar to the real bone, even if it presents some differences. There is not the presence of the medullary canal, and it is a little bit geometrically different. However, as in the human body, it consists of a solid part that represents the spongy bone and a coating shell part, the cortical bone, but, unlike the real clavicle, it is characterized by a constant thickness of 1mm. As the costal cartilage, the cancellous bone is modelled with hexahedra elements, using the element formulation 1, and with material 105. Material 24, MAT_PIECEWISE_LINEAR_PLASTICITY, is chosen for the cortical shell, an elastoplastic material for which is defined stress-strain parameters.

The ligaments, which colleague the clavicle to the sternum and scapula, are modelled as shell parts without recreating the whole joint. As the cortical bone, the AC ligaments are modelled with material 24, but in this case, no stress-strain curve is defined. The SC and coracoclavicular ligaments are characterized with material 34, MAT_FABRIC, usually used for the airbag and set to avoid excessive compressions. This type of material allows to set two different Young's modulus, introducing more rigidity, but only the one for longitudinal direction is defined.

3.2 Abdomen organs

Liver and spleen are among the internal organs most at risk during impacts. A better analysis and introduction of them is needed to improve the model.

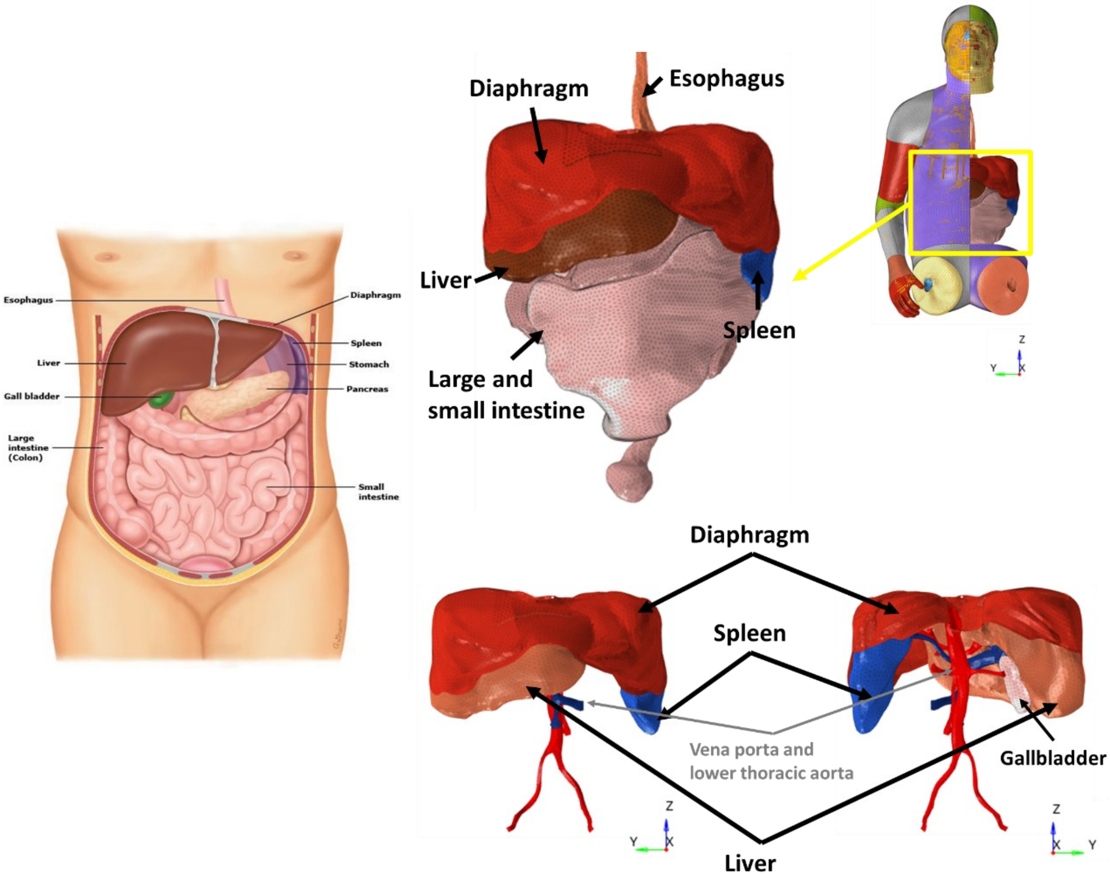

Figure 20 - Liver and spleen representation in the human body [13] (left) and in the THUMS (right)

3.2.1 Liver

Located on the right side of the human body, under the diaphragm, the liver is the heaviest abdomen organ with about 1.5kg. It is one of the vital organs dues to clean the body from metabolites and old red blood cells and produce bile to digest fats [12, 13].

The liver is divided into two lobes, connected by the Glisson's capsule, a fibroelastic connective tissue layer containing the liver. It is also divided into other 2 lobes in the inferior part: the caudate lobe and the quadrate lobe.

Even the surface is not homogeneous; where the liver faces on the diaphragm, the organ is in direct contact without a coating as an interface. On the contrary, the peritoneum covers the visceral surface; except for where the liver links to the gallbladder and the porta hepatis. This serous membrane must reduce friction against other organs, and it creates folds that are the falciform ligament, to link the abdominal wall, and the triangular ligaments, to link the lobes to the diaphragm.

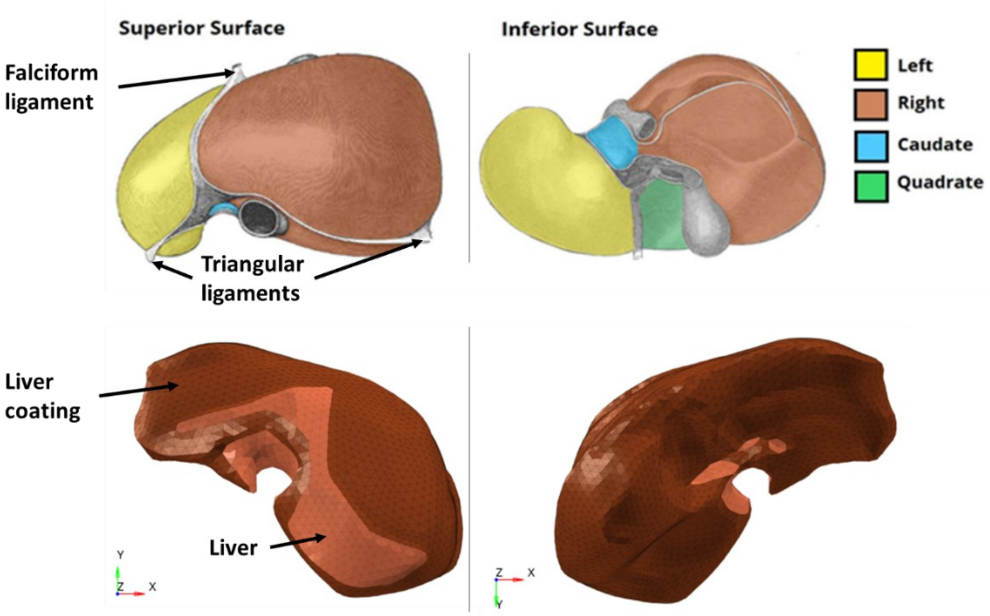

Figure 21 - Liver representation in the human body [13] (left) and in the THUMS (right)

As the thoracic organs, the liver is simplified in THUMS. It is composed of one homogeneous organ covered with a shell part. Both parts, the solid one and the shell, are modelled with tetrahedra elements. Formulation 13 is used for the solid and the 4th for the shell. The material 181, MAT_SIMPLIFIED_RUBBER is chosen to recreate the liver and material 34, MAT_FABRIC for the coating, usually used for the airbag and set to avoid excessive compressions.

3.2.2 Spleen

Located in the left side of the human body, under the diaphragm, the spleen occupies the space under the ninth, tenth, and eleventh ribs as figure 22 shows. Moreover, two ligaments connect the spleen to other organs. The Gastrosplenic ligament, made of folded peritoneum, allows the anterior spleen-stomach connection. The Splenorenal one provides the posterior spleen-left kidney contact (figure 23) [12, 13].

Spleen is one of the lymphatic organs, and it has several roles. It works as a filter, deleting old red blood cells and it is also important for the active immune response using humoral and cell-mediated responses. Splenic artery and vein take care of spleen sustenance and drainage.

It is an organ that can enlarge, a phenomenon called splenomegaly caused by many diseases and disorders. Normally spleen is not palpable, but during this circumstance, its dimension varies, up to occupy a vast region of the left side of the abdomen. It is usually in a range of 7cm to 14cm in length and almost 230g in weight, considering men 160cm-199cm height. When splenomegaly occurs, the spleen measures more than 20cm in the most dangerous situation.

THUMS's spleen is modelled with hexahedra elements using the formulation 13 for the section. Like the liver, the material 181 is used and even the coating has the same characteristics as the liver's coating.

Dimension is very different from the real ones. As figure 22 shows, it is located not only under the ribs but stands out beyond. It is almost 510g in weight and 17cm long. This condition would indicate a "Moderate splenomegaly" in the human body.

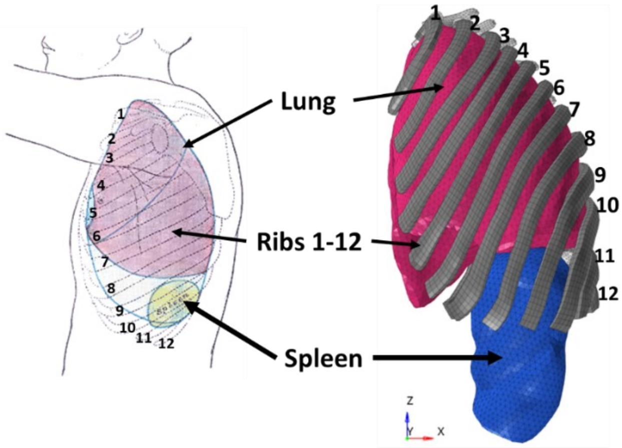

Figure 22 - Spleen representation in the human body [12] (left) and in the THUMS (right)

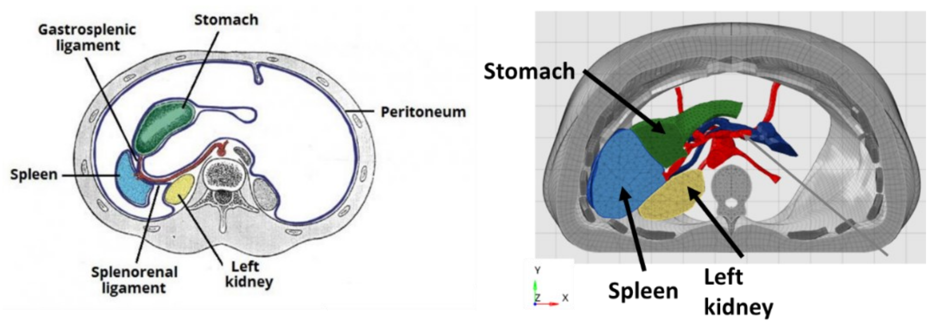

Figure 23 - Spleen contacts representation in the human body [13] (left) and in the THUMS (right)

Chapter 4

PEAK VIRTUAL POWER METHOD (PVP), ABBREVIATED INJURY SCALE (AIS)

This thesis originated with one goal, continue Professor Bastien's work on obtaining an acceptable AIS (Abbreviated Injury Scale) score for two abdominal organs included in the FE model of the human body, the liver and the spleen. The scores should then be compared to the medical reports of the real-life accident: the more similar they are, the more the model is accurate.

The real-life accident is based on the CIREN database; the sled model, shown in figure 24, is born to recreate the same situation. It was recreated using THUMS and the second-row seat to simplify the reconstruction. Unlike the first-row occupant, the airbag is not necessary, it would also reduce the level of injuries. Neither an accurate vehicle interior geometry is needed because only the front seat, with which the body impacts, is necessary.

Figure 24 - The sled model

Since the purpose is to find AIS value, it is important explain what this code is. It was created by the Association for the Advancement of Automotive Medicine to classify injuries' severity. It is an international code that indicates the part of the body considered and the type of injury and assigns a score from 1 to 6 to quantify the severity (Figure 25). These evaluations are used to understand the mechanism of injury to improve the safety of the vehicle [27].

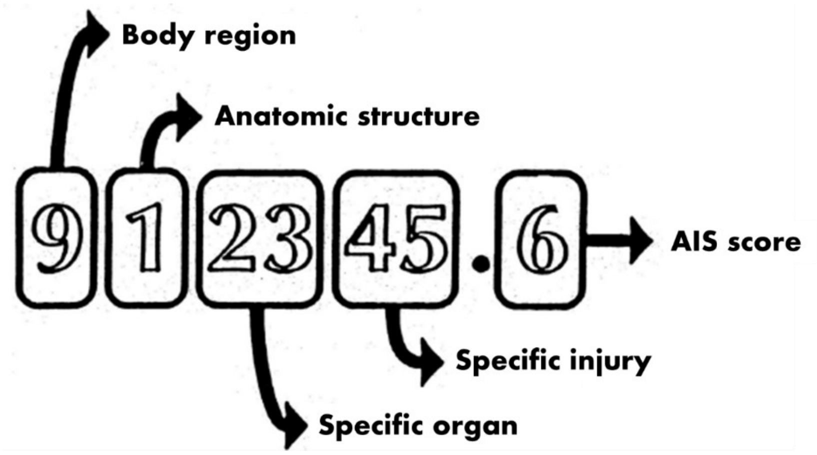

***Figure 25** – The AIS code example*

Injuries cause tissue deformation, for this reason, strain is always considered when they occur. Indicators based on strain already exist and are used, but they are not useful for trauma location.

An innovative energy-based injury criterion, the Peak Virtual Power (PVP), was proposed and it could be used to overcome these limitations and to obtain the AIS score for the sled model to compare it with the real one. This criterion, derived from the rate-dependent form of the 2nd law of thermodynamics using the Clausius-Duhem inequality, bases on the consideration that irreversible work in a human body represent the injury [28].

PVP method consists of multiply the stress and strain rate, identify and memorize the maximum value for all the time history of the impact. After all, the greatest value among those stored will be used to codify the AIS score from AIS corridors, indeed PVP is proportional to the AIS as equation 1 reports:

$$PVP \propto AIS \propto max\ (\sigma \cdot \dot{\varepsilon})$$

***Equation 1** - Peak Virtual Power (PVP) formulation [28]: σ is the stress and $\dot{\varepsilon}$ is the strain rate*

Finally, PVP corridors are necessary to obtain the AIS score for the interested organs. These corridors are “PVP-impact velocities curves” and each one represents different AIS levels. Sled model is simulated for different impact velocities, the AIS 4 corridor is built, and this one is used to calculate the remaining curves. The AIS 4 curve is generated taking the PVP value of the interesting organ, using its first element that reaches 30% of the strain, the equivalent to the AIS 4 level. The same procedure is followed for the other impacts simulated with different velocities. Finally, the points are interpolated to obtain the curve.

Next, the other corridors are calculated using equation 2 and corridors in figures 26-27 are drawn to extract the AIS score thanks to the maximum PVP value stored in the previous step.

$$PVP_{AIS-A} = PVP_{AIS-4} \times \frac{A_{AIS-A}^3}{4^3}$$

Equation 2 *- Equation for AIS from 1 to 5 (A) [28]*

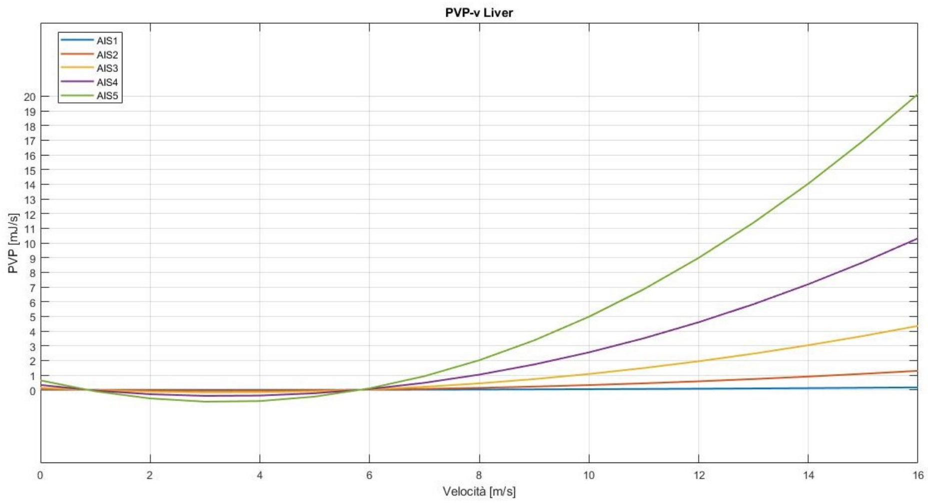

Figure 26 *- AIS corridors for the Liver*

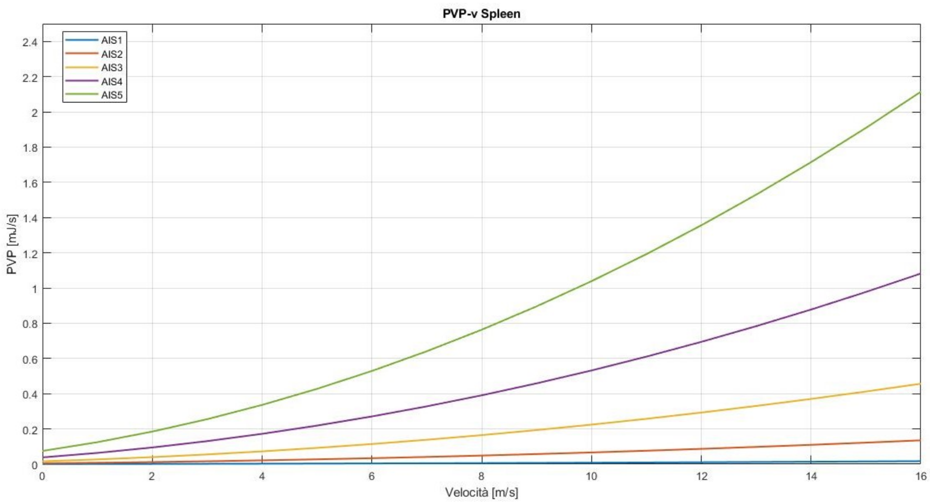

Figure 27 *- AIS corridors for the Spleen*

Since previous works found AIS score too different than those associated with the real accident, sled model’s improvements have become necessary. Many parts of the model are to be improved, but this thesis work focuses on THUMS' changes, presented in chapter 6, to make it more similar to the human body.

Chapter 5

THUMS VALIDATION

The first step of this thesis work is the validation of a version of THUMS, the original Academic Version 4.02 AM50 Occupant model, provided by Politecnico of Torino. It is important that the model turns out to be stable and reflects human body properties. It means that the model, if unchanged, must not suffer changes in performance running the same simulation several times and as previously discussed, the extracted curves shall fall into corridors.

THUMS is used in torso impacts presented in chapter 2. The simulation is run using LS-Dyna/9.3 as solver, with single precision. For every impact, the energies are checked, and force and deflection curves (Rerun in the figures) are compared with corridors and curves from Professor Bastien simulations (THUMS in the figures) to verify the model's stability too. SAE filter in seconds, with a frequency set on 180Hz, was used to obtain force curves in all validation tests.

5.1 Thorax validation

The first impact validation is focused on the thorax and as presented previously, there are three types of impacts.

5.1.1 Frontal impact

The total energy absorption is shown (figure 28). The kinetic energy reduces its value, but it does not reach 0J: this depends on the fact that the simulation stops before the body can collapse on the back, an effect that does not need to be analyzed (see chapter 2).

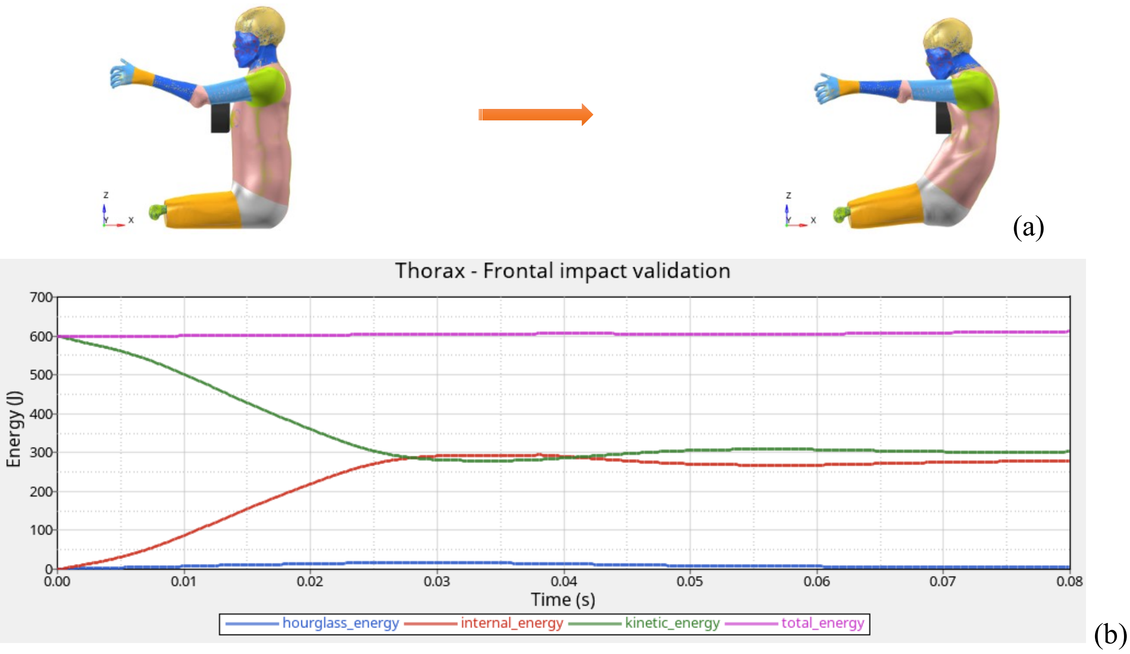

Figure 28 - Thorax - Frontal impact representation (a) and energy curves (b)

Impactor's force vs Chest deflection's curves are plotted in figure 29. Running again the simulation, the results almost follow the original ones: this means that THUMS performances are unvaried, and the model is stable. The discrepancies can be caused by the filter, or the possible different version of the solver used.

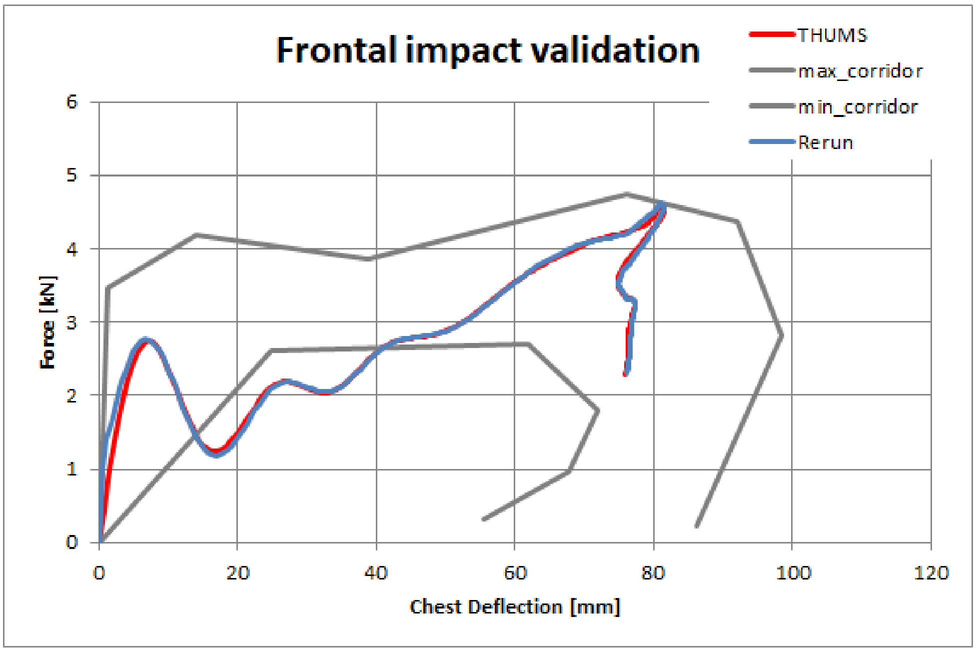

Figure 29 - Force vs Chest deflection for frontal impact

5.1.2 Belt impact

The belt impact case is different from the frontal impact previously analyzed. This time THUMS is positioned on a table, and when the belt impacts the body, it is stopped by the table itself. As the simulation goes on, the effects of the strap become visible on THUMS. This is the reason why in the graph all the energies start from 0J as opposed to thorax frontal impact (Figure 30). During the simulation, kinetic energy will decrease when the body begins to oppose the deflection and total energy maintains constant in the last part of the simulation.

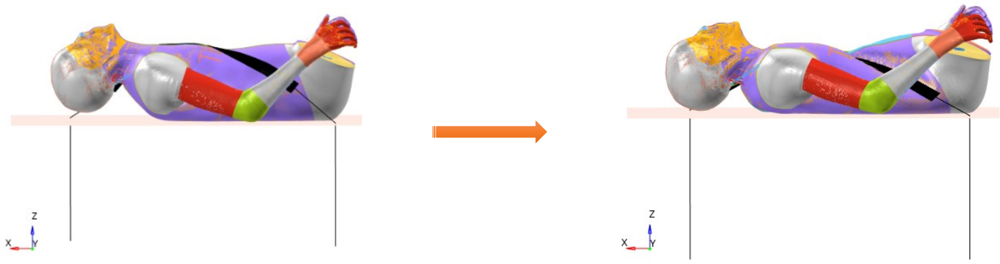

(a)

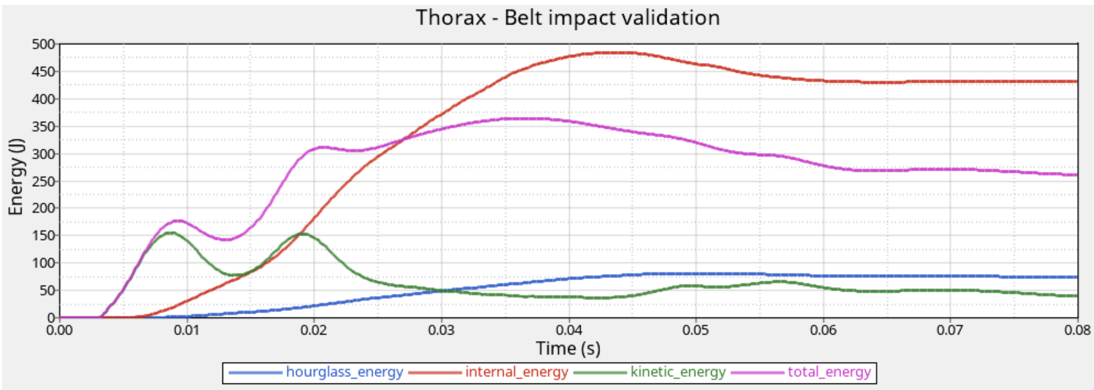

(b)

Figure 30 *- Thorax - Belt impact representation (a) and energy curves (b)*

Deflection curves for the point of the torso are extracted, as for the experimental test. Figure 31 shows that there are nodes, and so different areas of the thorax, that result in too stiffer or too little rigid. Nodes 4, 5 and 6, which are on the left side of the thorax, do not respect corridors and the deflection in these points is greater than the real one. On the contrary nodes 7 and 8, on the right side, are less deflected than the normal but, while node 8's curve is a little different from the corridor (falling in the max-min zone), node 7 represents a stiffer zone because its curve is out of range.

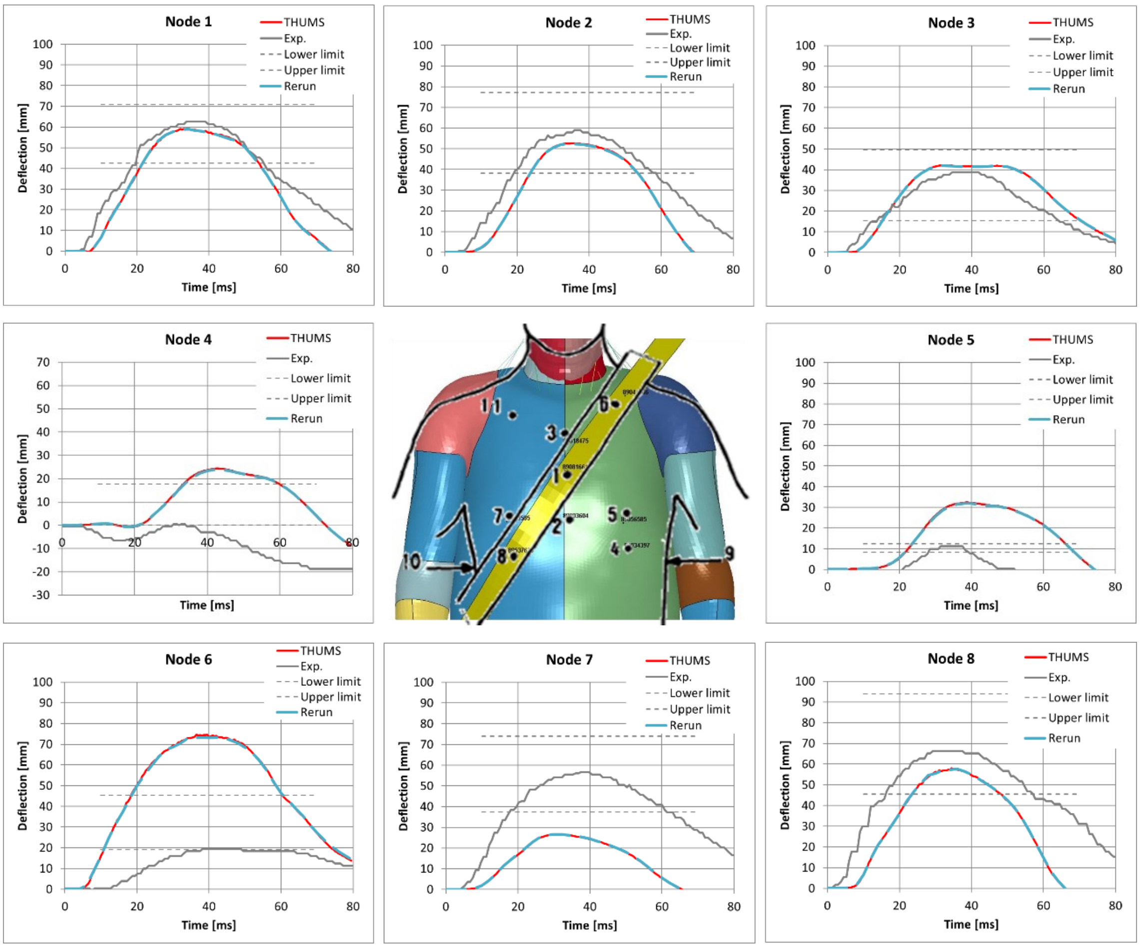

Figure 31 *- Deflection curves for THUMS' nodes*

5.1.3 Lateral impact

In lateral impact validation, the situation is very similar to frontal impact. The kinetic energy decreases slowly, indeed in the last part of the simulation the curve seems to increase again (Figure 32). Therefore, the total energy remains almost constant at the beginning, then the curve grows. This problem could be due precisely to the thrust that the impactor gives to the chest when it hits it. As in the frontal impact, the situation is analyzed until the load no longer acts and the kinetic energy's curve does not reach 0J.

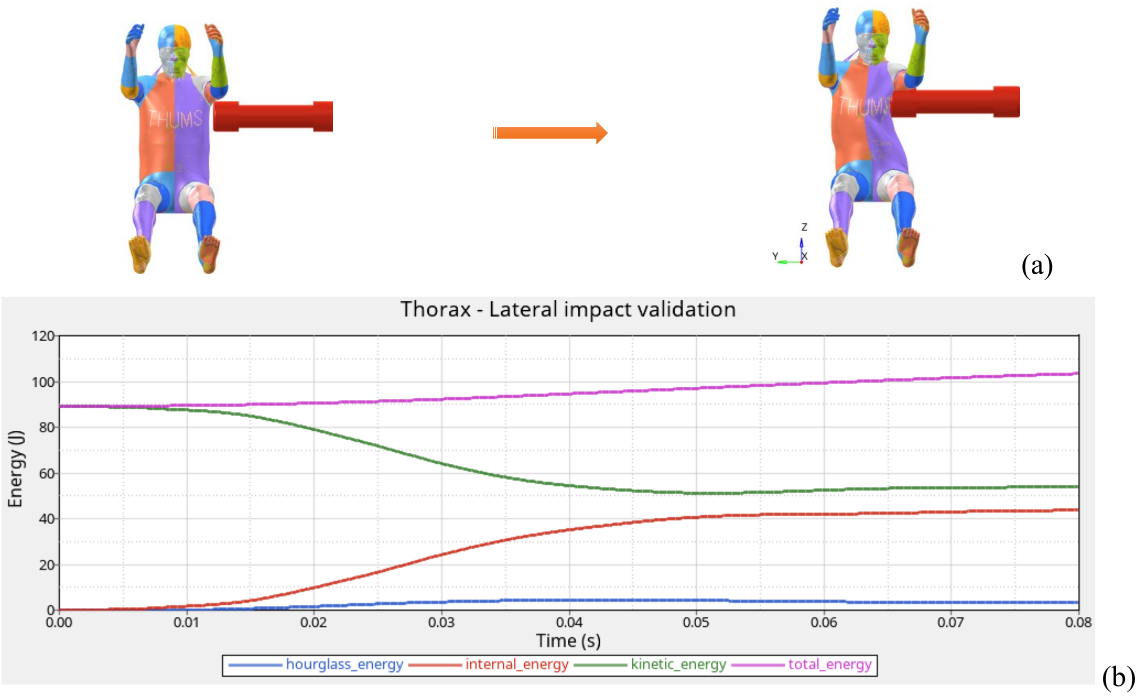

Figure 32 - Thorax - Lateral impact representation (a) and energy curves (b)

Force and Chest deflection are compared with the original curves in figures 33-34. Curves are practically overlapping, and they fall into corridors.

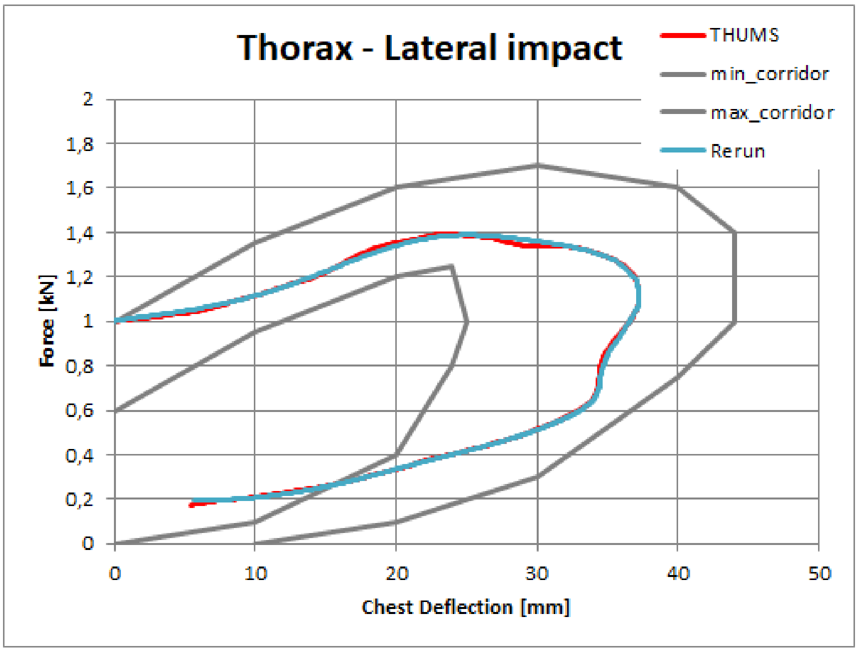

Figure 33 - Force vs Chest deflection curve for lateral impact

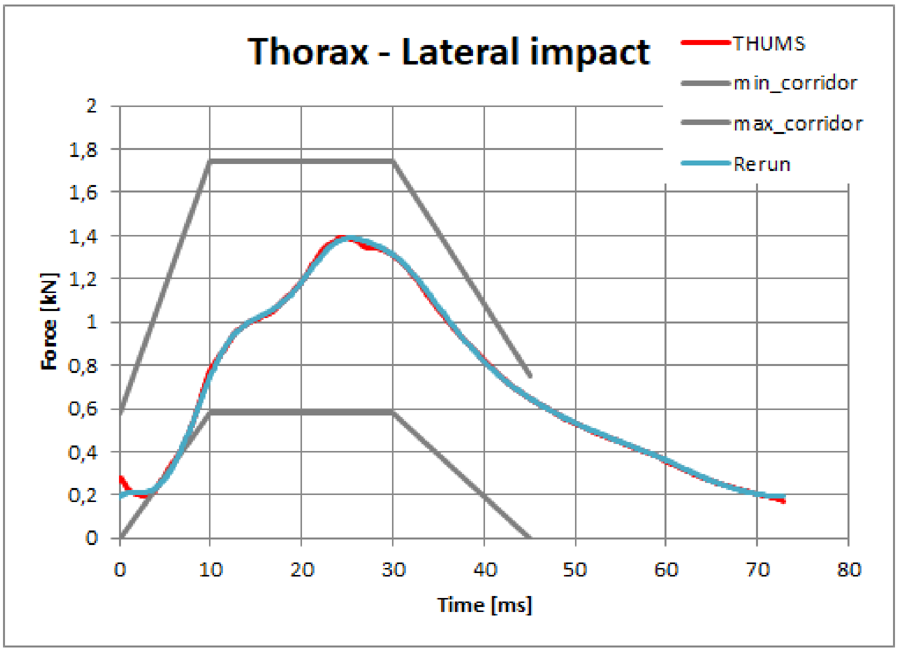

Figure 34 *- Force curve for lateral impact*

5.2 Abdomen validation

As shown in chapter 2, the abdomen is the second area tested to understand the bio fidelity of the THUMS.

5.2.1 Bar impact

As before cases, kinetic energy decreases and internal increases, while the total one maintains constant (Figure 35). As always, in the validation impacts, what is interesting is the impact itself and not what happens after that. For this reason, as in the frontal impact case, kinetic energy does not achieve 0J.

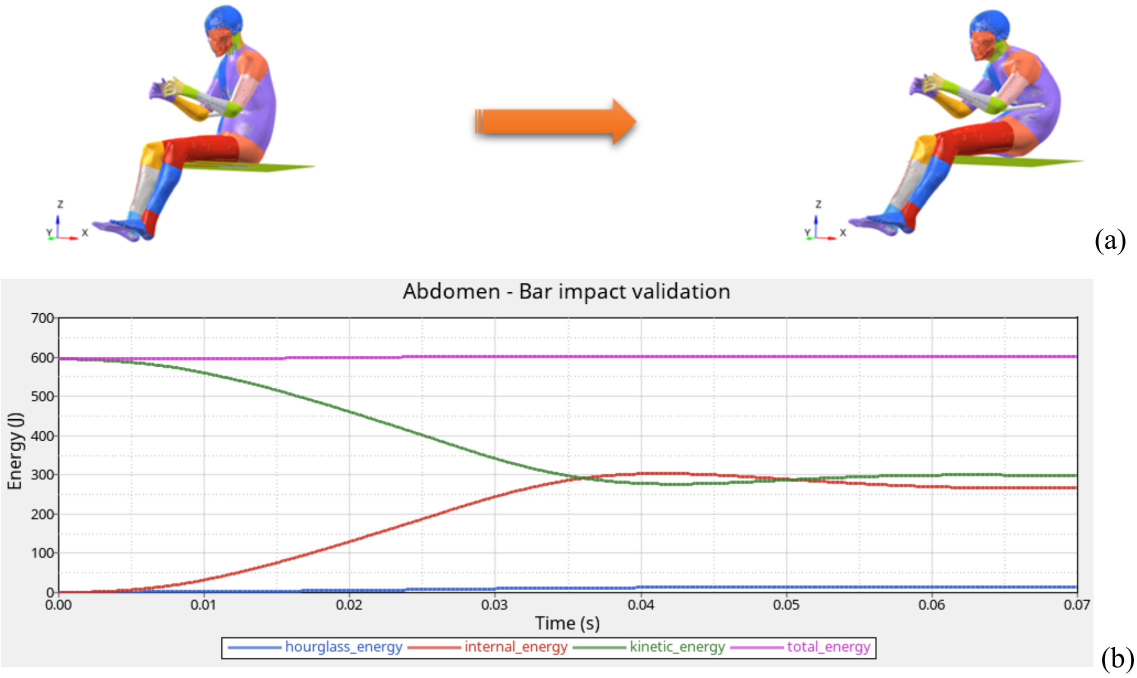

Figure 35 *- Abdomen - Bar impact representation (a) and energy curves (b)*

Once the impact is simulated, x-force, between impact bar and the THUMS, vs bar stroke is displayed in figure 36. The THUMS is stable, being the curves superimposed and it falls for the most part into corridors, except for the peak. It may be due to not perfect modelling of the abdomen and its organs, or to the type of the impactor, the rigid bar.

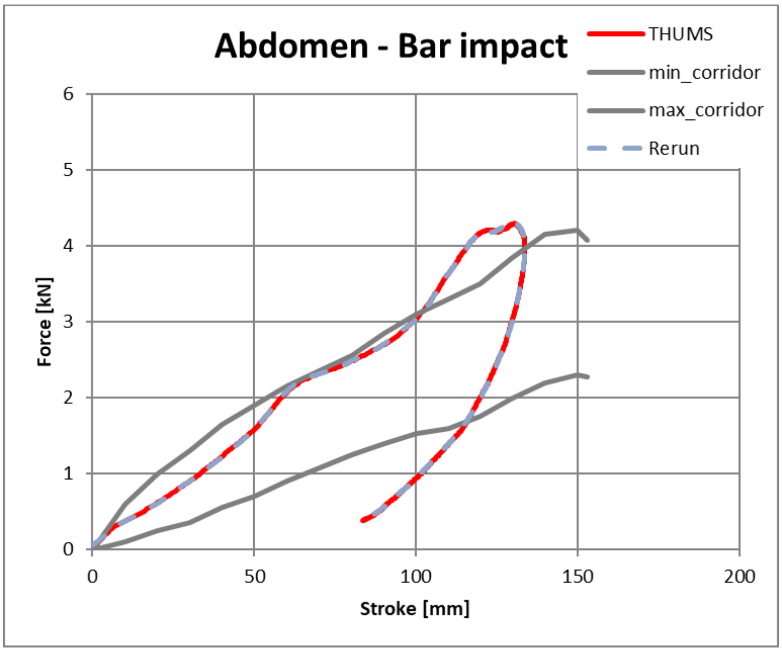

Figure 36 *- Force vs chest's stroke curve for bar impact*

5.2.2 Belt loading

Energy validation, for belt loading in the abdomen, is similar to the one for thorax-belt impact. The two impacts are similar, but this time the belt focuses only on the abdomen. In addition, this time, the hourglass is less prevalent than in the thorax case (Figure 37).

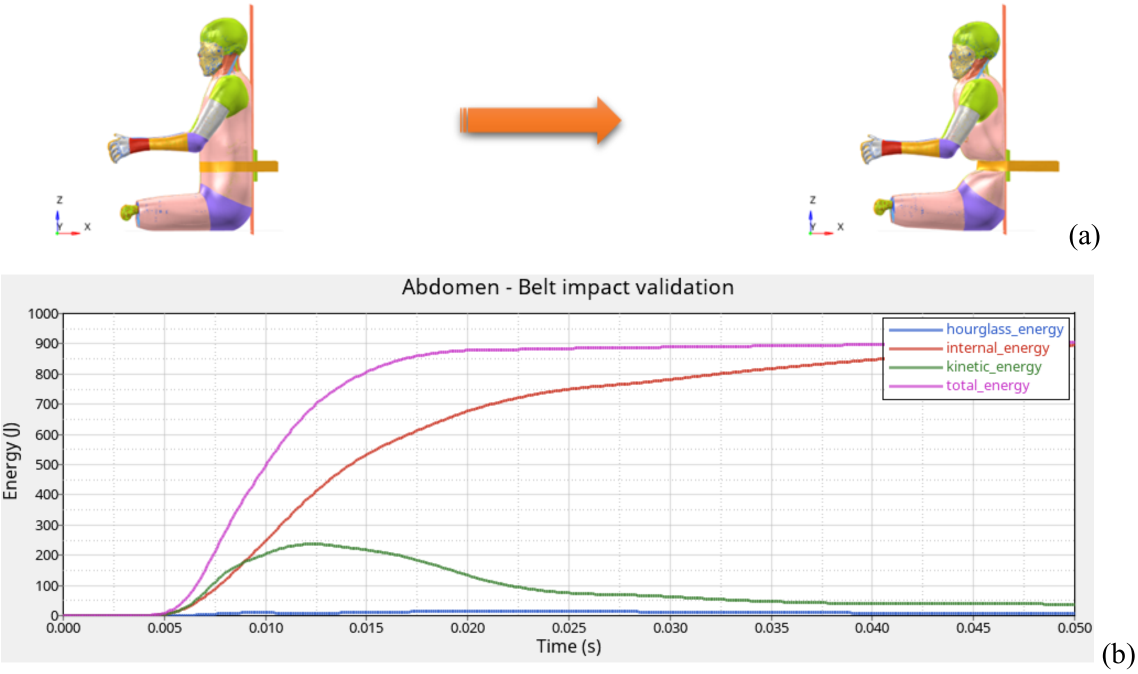

Figure 37 - Abdomen - Belt impact representation (a) and energy curves (b)

X-force - belt stroke's curve is then made and despite some discrepancies, it can be said that even for this impact the THUMS results stable, and the curve fall into the corridors (Figure 38).

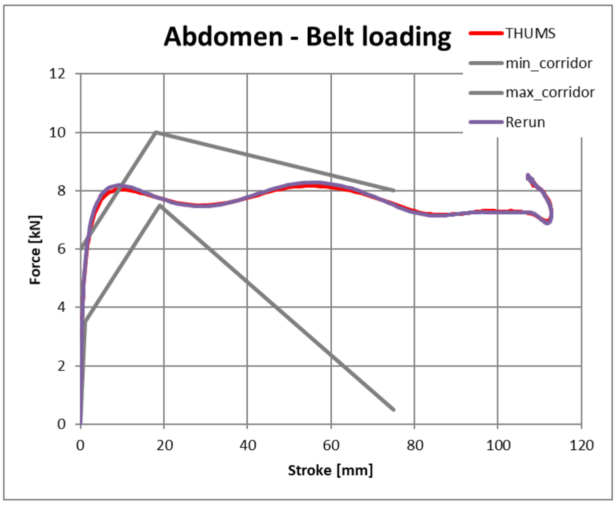

Figure 38 - Force vs chest's stroke curve for belt impact

5.3 Pelvis validation

As presented in chapter 2, the last part of the body tested for validation, is the pelvis area.

5.3.1 Knee-thigh-hip impact

Validation of the knee-thigh-hip impact is divided into three simulations, as explained in chapter 2. The trends are the same that other impacts and as velocity increases, similarly, kinetic energy does (Figure 39).

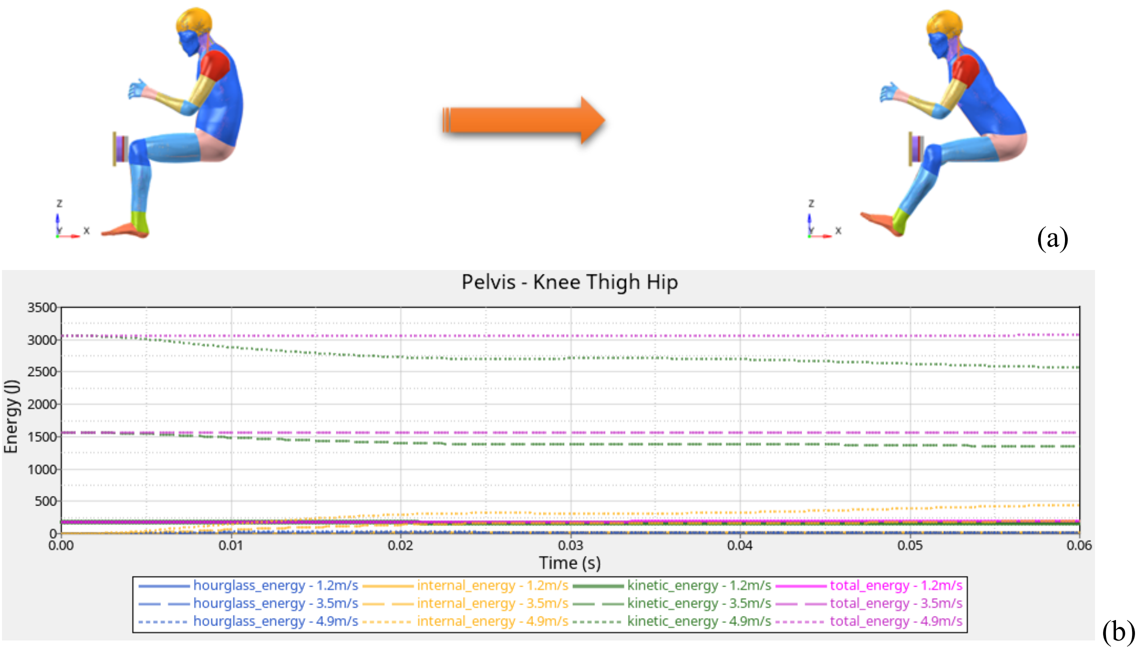

Figure 39 *- Pelvis - Knee-Thigh-Hip impact representation (a) and energy curves (b)*

Filtered x-force, obtained from the average outcomes of the loadcells, is then compared to corridors and THUMS curves in figure 40. Once again, the model is stable and curves, even if differ somewhat, follow corridors trend.

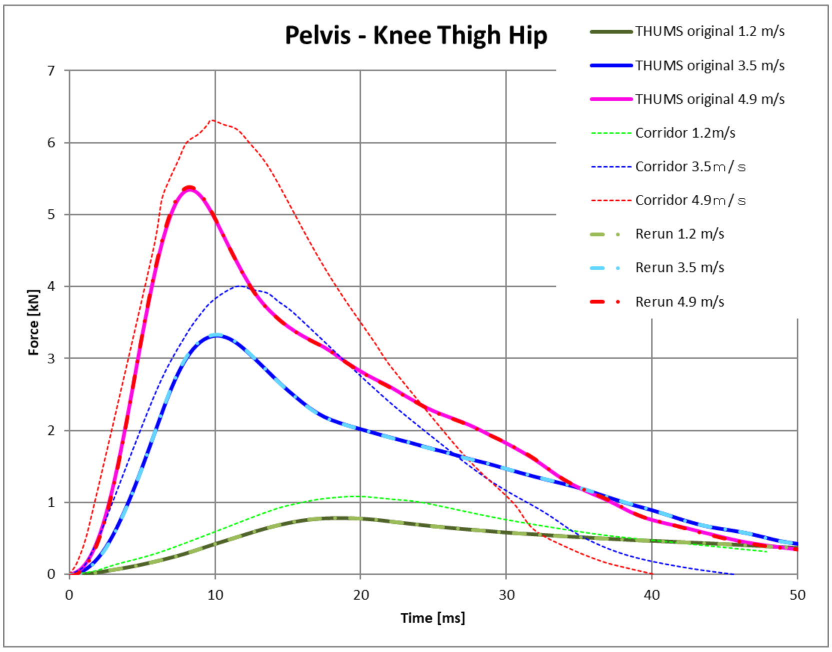

Figure 40 - Force curves for Knee-Thigh-Hip impact

5.3.2 Acetabulum lateral impact

Energy comparison for this impact is shown in figure 41. In this case, two types of simulation are run, changing failure parameters. In the case called Failure strain 3%, the failure and strain rate (C and P) parameters of material's cards are respectively defined as 2.8E-2 strain, 360.7 strain /s and 4.605 strain/s. These values are then changed for Failure strain 1%'s case, setting FAIL to 5.0E-3 strain and, C and P to 0 strain/s.

Kinetic energy decreases in both cases, but when failure options are reduced, kinetic energy continues to fall until 0J. This means that failure parameters can influence a lot the material properties and model performances.

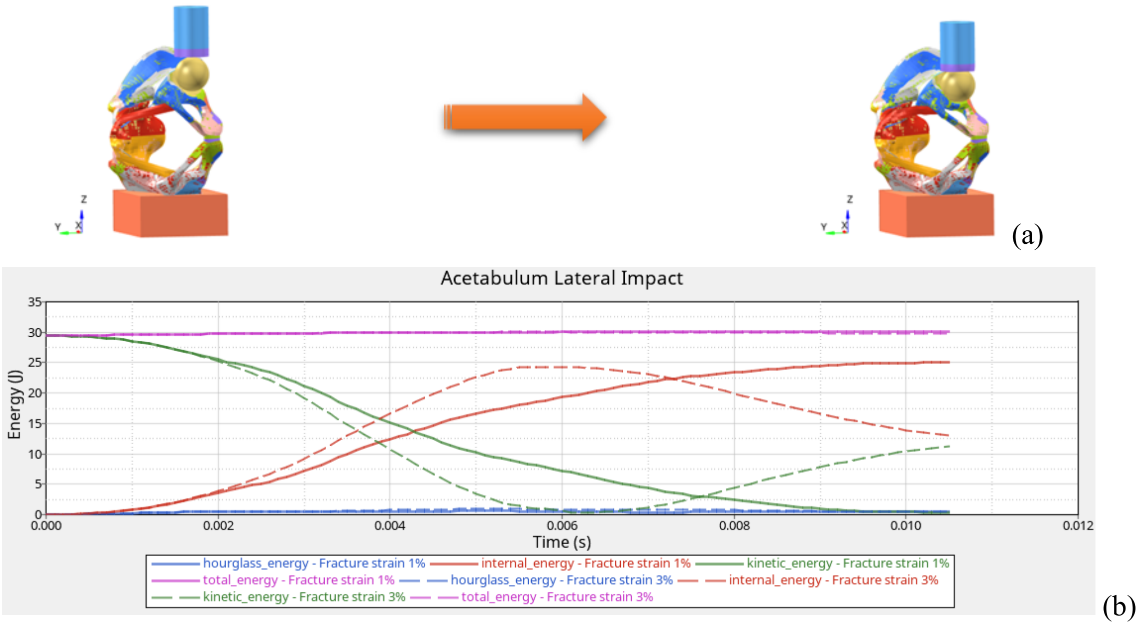

Figure 41 *- Pelvis - Acetabulum lateral impact representation (a) and energy curves (b)*

Impactor vs sphere force is displayed in the graph below (Figure 42). Both curves are into the corridors for more than half simulation, in the last part, they come out of the range. Moreover, fracture strain 1%'s curve differs from Professor Bastien simulation's curve, but having the same trend, the model is considered stable the same.

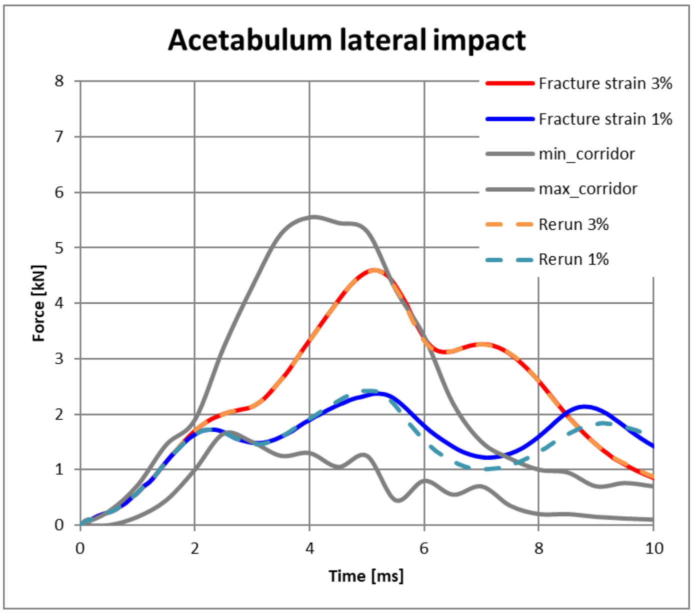

Figure 42*- Force curves for Acetabulum impact*

The model respects real performance in almost all tests, falling in the interval limited by corridors. Great deviations are found only in the thorax belt impact, but this is enough to understand that the THUMS does not reflect the actual behaviour of the human body.

One of the purposes of this thesis is to try to apport changes in the THUMS in order to have a biofaithful model. It is possible to obtain such a result by improving the properties of the organs described in chapter 3, verifying if, those changes, have a positive or negative influence on the model (Chapter 6).

Chapter 6

CHANGES IN THE THUMS

The reasons why the organs, described in chapter 3, are taken into account, to make the THUMS more accurate, are discussed in this chapter. In addition, the changes that have been attempted to obtain an accurate model, are presented, evaluating their influence on THUMS behaviour.

There are some organs that can affect THUMS performances observing the model. Figure 43 shows the thoracic area of the model in the belt impact, the one for which curves, in indicated nodes, were out of range (chapter 5). Moreover, the organs previously considered are shown, including thoracic ribs whose modifications are discussed in Giulia Mondino's thesis [29].

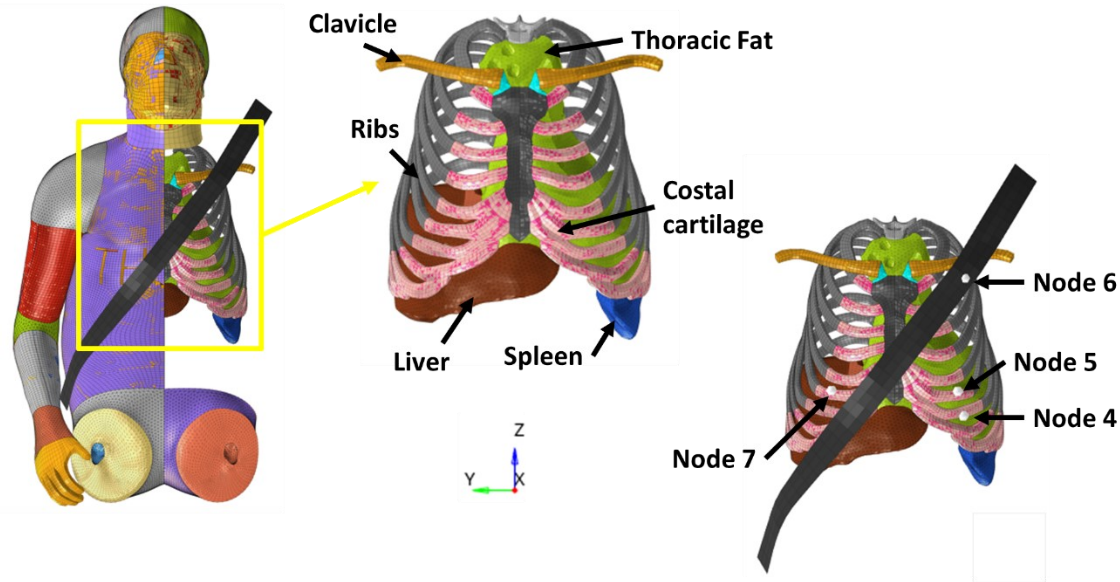

Figure 43 - Organ's representation in THUMS for thorax belt impact

Unlike the costal cartilage, clavicles and thoracic fat, the liver and spleen do not belong to the thoracic cage. However, since they are among the internal organs most at risk during impacts, they were chosen to be evaluated with the PVP method in professor Bastien's work. For this reason, improvements will be considered in this study.

6.1 Costal cartilage

The first attempt is to try to analyse the material cards used for the organ from which deflection curves, for the problematic belt impact, are extracted: costal cartilage, shown in pink in figure 44, with also the nodes to which reference is made.

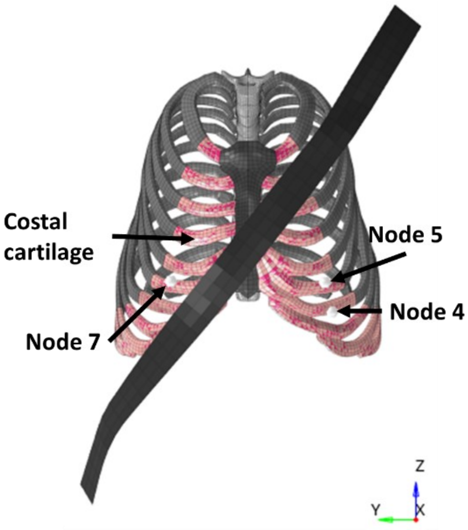

Figure 44 - Costal cartilage in THUMS with the belt and problematic nodes

Ribcage has always been taken into account for years, but despite ribs and other parts were well-characterized, costal cartilage has been somewhat neglected. However, the costal cartilage represents the mechanical coupling for the ribs and the sternum, for this reason, a more accurate analysis for this organ is presented in this study.

As mentioned in chapter 3, the costal cartilage in THUMS encloses only the matrix properties, the cartilage substance, nevertheless, the perichondrium should be represented too to have a more realistic model. Considering its position and its different composition, this matrix coating could have a great effect on the biomechanical response of costal cartilage.

Forman et al. [30, 14] were among the first who investigated the perichondrium role through structural tests, which consists of applying to a single segment from the sternum side, a load directed to the posterior. The perichondrium lack could decrease the stiffness of the model by 50%, influencing the entire ribcage deformation. A perichondrium representation could allow avoiding force peak on the substance.

The idea is to modify the costal cartilage model, representing not only the matrix but the perichondrium too.

Forman et al performed spherical indentation tests on the fourth costal cartilage, the longest single segment, of medium age men, without the perichondrium. A medium value of 11.1MPa is determined for the elastic modulus of the matrix [31] [14]. Next, they used specimens in cantilever-like loading and recreated the same conditions with the FEM, using a simple linear elastic material. Results suggest that this model well reproduce costal cartilage behaviour with an error range of 1-36%. This is a very small value if it is compared with the 50% of error from the point of view of stiffness due to the lack of the perichondrium.

However, this model is not completed without the perichondrium. Forman et al. [30], also tried to model this element using a shell part coating the matrix. Material 91, MAT_SOFT_TISSUE, is chosen, it is a transversely isotropic hyper-elastic material usually applicate for ligaments, tendons, fibrous, and collagen-based connective tissue. It requires a series of material coefficients (C_i) to define the energy density function displayed in figure 45.

$$W = C_1(\tilde{I}_1 - 3) + C_2(\tilde{I}_2 - 3) + F(\lambda) + \frac{1}{2}K[\ln(J)]^2$$

Figure 45 *- Energy density function for material 91: I_i first and second deviatoric invariants of the right Cauchy deformation tensor; F defines the material behaviour owing to the tensile stretch of the collagen fibres in the tissue; J is the volume ratio; K is the bulk modulus; C_i are material coefficients [30]*

Different assumptions were made. C2 was set to 0 because the perichondrium was considered as a Neo-Hookean material, and the bulk modulus (K) to 4GPa to model is incompressible behaviour. Other parameters were defined, with the purpose to recreate the force vs displacement curves obtained from structural tests briefly described above.

Hence, the changes are reported in THUMS, following Forman et al's model. The solid material is simplified passing from material 105, MAT_DAMAGE_2, to material 1, MAT_ELASTIC, decreasing the young's modulus from 29MPa to 11.2MPa. The perichondrium is modelled with the parameters described above using the existing shell element which coats the solid part. As in other organs in the THUMS, this shell was modelled with null material, hence used to better control, and simulate the contact with the other parts during the simulation.

The new model is run again to understand if changes have an influence on the response of the problematic simulation, the Thorax–Belt impact. Unfortunately, curves do not change, this is positive because means that the changes did not introduce instabilities, but these changes did not solve the stiffness problem as hoped.

The little literature present on this subject does not allow the creation of a more realistic model for costal cartilage yet. New research could be carried out in the future and perhaps discoveries will be useful in THUMS.

6.2 Thoracic fat's analysis

Under the thoracic cage, it is impossible not to notice the presence of the thoracic fat. This is predominantly present to the left side of the THUMS (Figure 46), were the nodes 4 and 5 are indicated. This might have something to do with the different behaviour between the two sides of the model, as found in Thorax–Belt impact validation in chapter 5. For this reason, a better comparison between the performances of the two sides is examined.

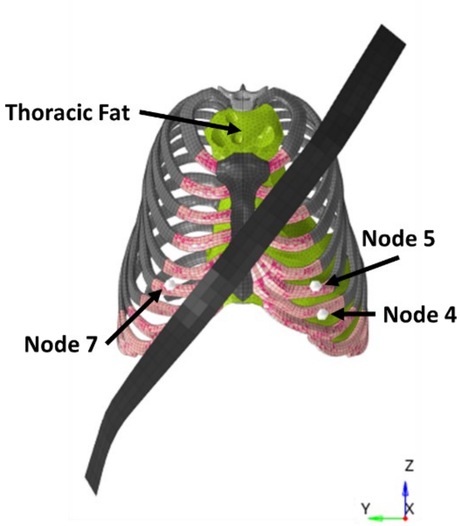

Figure 46 - Thoracic fat in THUMS with the belt and problematic nodes

The Thorax-Frontal impact is used as basis, indeed the impactor is positioned, first, in front of the left side of the chest, then at the right, as it is shown in figure 47.

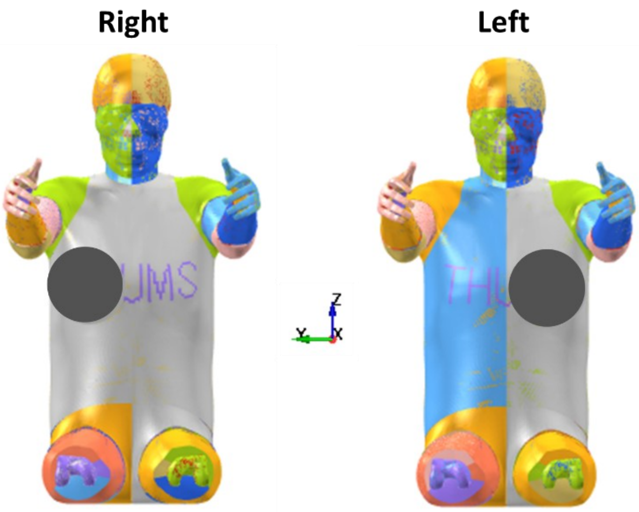

Figure 47 - THUMS with the impactors positioned on the left and rights side of the body

Force and deflection of the thorax curves are compared in figures 48-49 to understand if the THUMS reacts in the same way. The right side is more deflected than the left, where the presence of the thoracic fat is very high. The percentage difference is then calculated, the curve increases to almost 21.25%, indicating a not negligible difference.

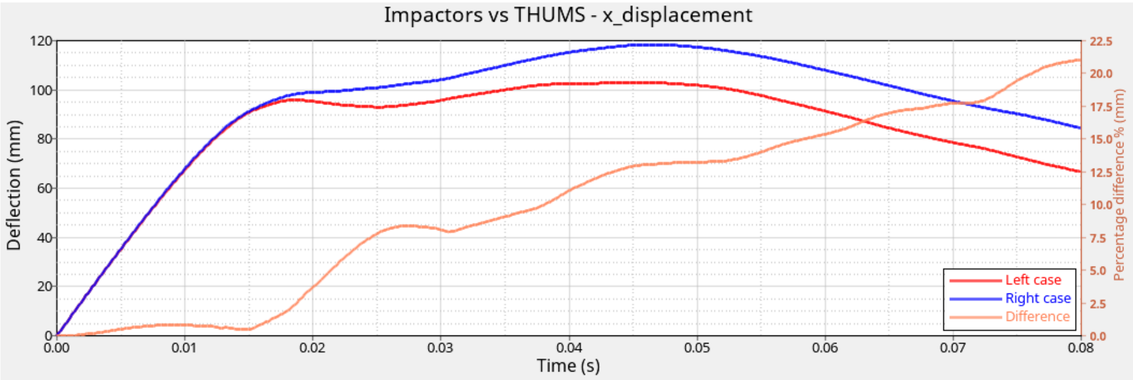

Figure 48 - Displacement curves for impactors simulations

Force curves also reflect this aspect, the percentage difference curves highlight moments in which there are the biggest discrepancies.

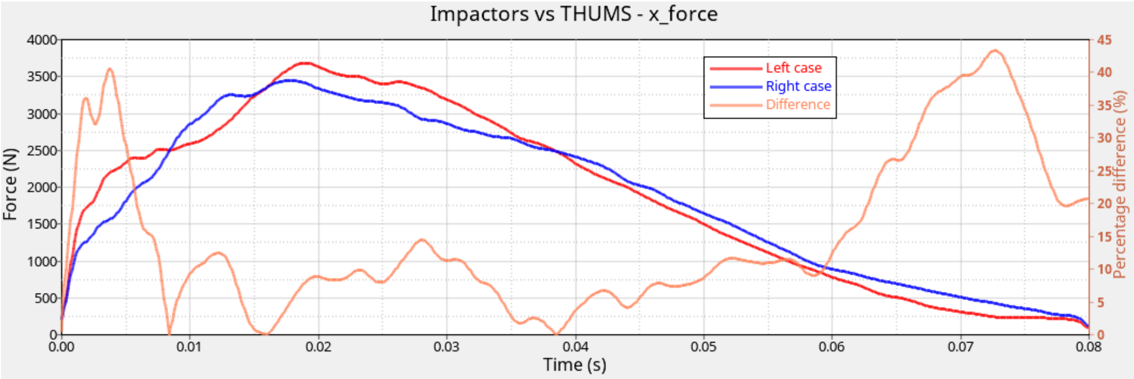

Figure 49 *- Force curves for impactors simulations*

These curves and concerning differences are the reason why a better investigation on thoracic fat's dimension is carried out in this thesis.

Thanks to its attenuation values, thoracic fat is easy to identify by computer tomography (CT) [15, 16, 17, 18, 19, 20, 21]. The manual or automated tracing of the hearth's borders allows the volumetric quantification of the adipose tissue. Scientists have managed to discriminate between the epicardial and pericardial fat. They are represented under the unique name of thoracic fat in figure 50.

The figure makes it easy to understand the main difference between the real thoracic fat and its model in the THUMS, its dimension.

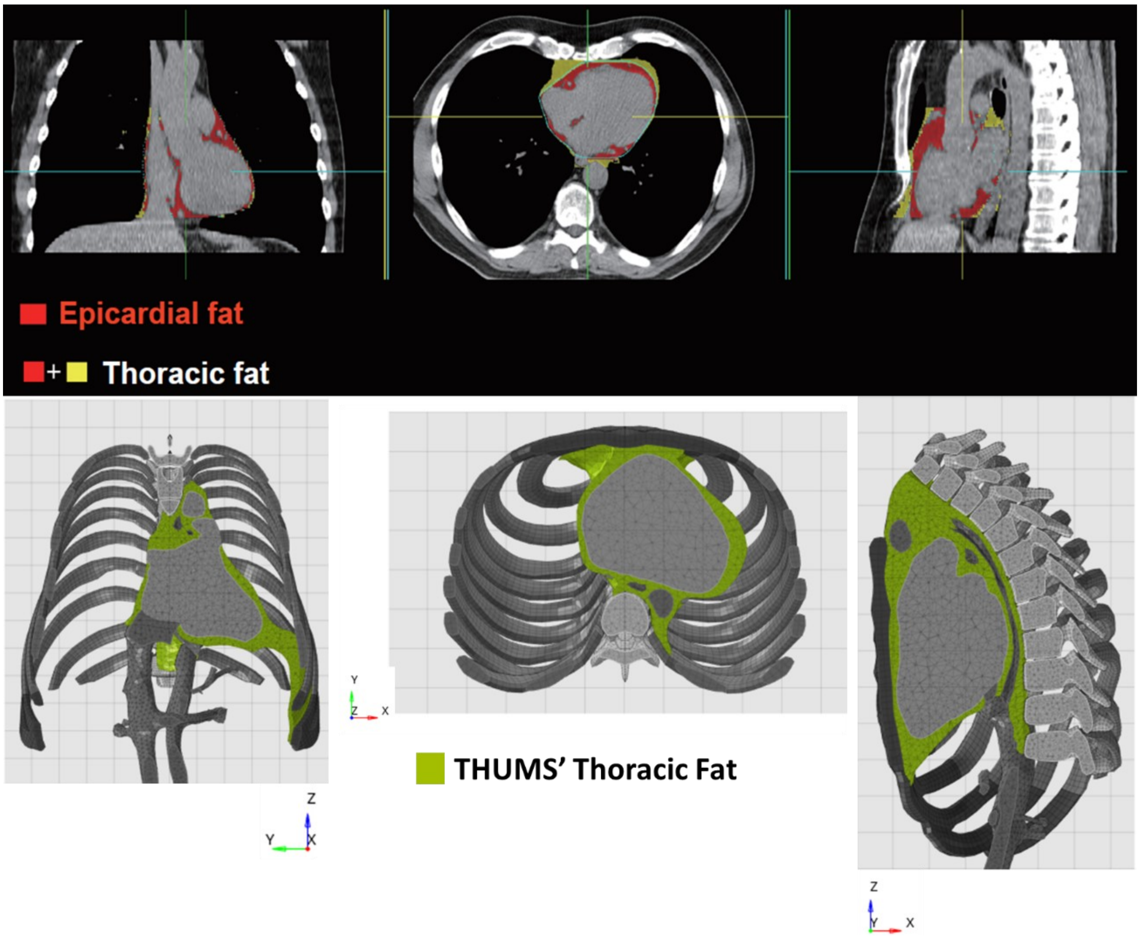

Figure 50 - Thoracic fat in the human body [15] and in the THUMS

Different research tried to calculate the volume of the thoracic fat. Regarding the epicardial fat, it covers 80% of the surface and is mostly situated in the right ventricular side. The separation from the pericardial fat has not been easy, the challenge was to identify the pericardium, which is very hard to detect, particularly in thin people.

Volume was then measured thanks to the segmentation. Epicardial fat is always in the range of 68cm^3 to 134cm^3, and Nakazato et al [15], also identified the value of 125cm^3 as the threshold for a healthy condition. Pericardial fat is less than epicardial one, it is in the range of 50 cm^3 to 70cm^3. As a result, the total amount of adipose tissue in the human chest is approximately in the range of 118-204cm^3, considering obese patients too.

Thoracic fat's dimension in THUMS is very different than CT values, the volume calculated in LS-DYNA is 805.03cm^3, with a percentage difference of almost 75%.

An option for future works could be trying to reduce the thoracic fat's dimension, rescaling this element with a more realistic value and test the impacts again.

6.3 Clavicle and its ligaments

The clavicle is taken into account, in this thesis work, for the same reason as the costal cartilage. Displacement's curve in node 6 is out of range in Thorax – Belt impact. The node does not belong to the clavicle, but it is in correspondence with the palpable bone as it shown in figure 51. A better analysis of this bone is carried out to make the bone more bio faithful.

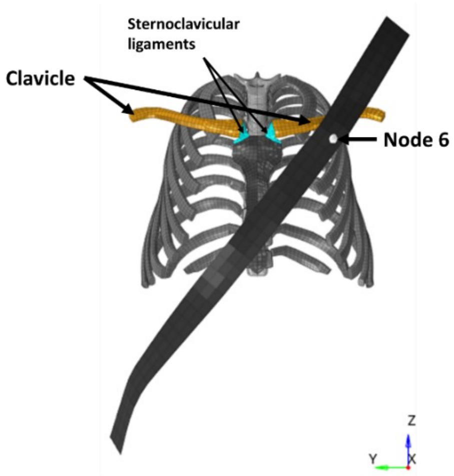

Figure 51 *- Clavicle representation the ribcage with the nodes and interested node*

Basing on literature, variations on material properties of the cortical bone are considered. Different studies state that cortical thickness is variable along the bone and similarly Young's modulus has different values according to the concerned area [26, 32, 33].

Firstly, the modification of the shell thickness is taken into account. The model presented a constant cortical thickness (the shell part) of 1mm. According to the articles, the bone is thicker in the middle, the area in which tensions concentrate when the clavicle is stressed, and thinner in lateral and medial ends, especially on the inferior side. The changes are made based on cortical thickness distribution reported in Z. Li et al. 2012 [26]. Both bones are modified considering each clavicle face and trying to recreate the same map reported in the article (Figure 52).

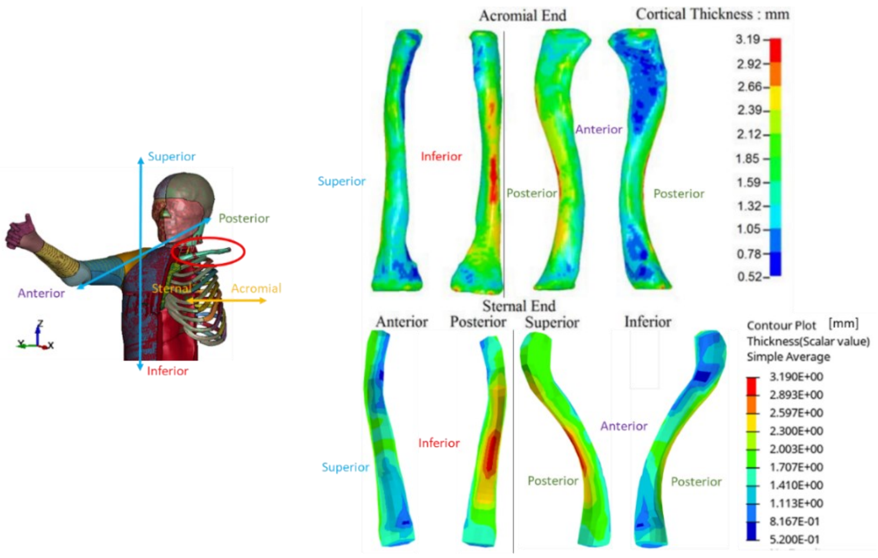

__Figure 52__ - Cortical thickness distribution in human body [26] (above) and THUMS reproduction (below)

Secondly, Young’s modulus variation is attempted too. As in the thickness's case, the elastic modulus was constant in the original model, set on 1.3020 GPa. Researchers found that it is variable along the bone, indeed the clavicle is more elastic where ligaments connect it to other bones and stiffer in the middle area. Z. Li et al. 2012 [26] also shows Young’s modulus distribution. Even in this case, the map is recreated for the THUMS. The clavicles are divided into different parts to make this, and for each part, different material properties are imposed (Figure 53). Following this method, the modelling is quite complicated because the mesh is less fine than that of the article and, therefore, it is difficult to make a homogeneous shell

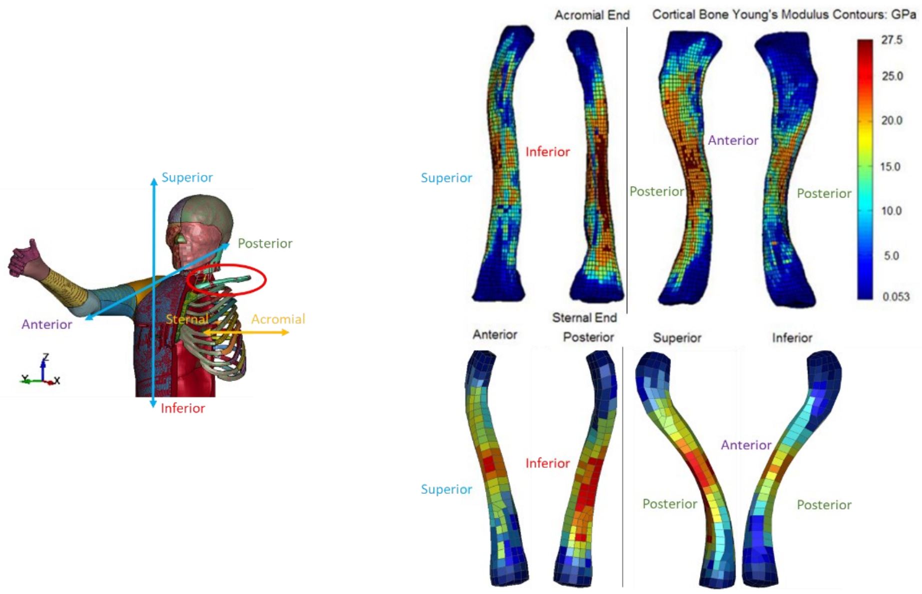

__Figure 53__ - Young's modulus distribution in human body [26] (above) and THUMS reproduction (below)

Finally, both clavicle models are tested in Thorax – Belt impact to understand if these changes can have influences on displacement curves. The modifications did not introduce instabilities, but the curves do not change the trend (Figure 54).

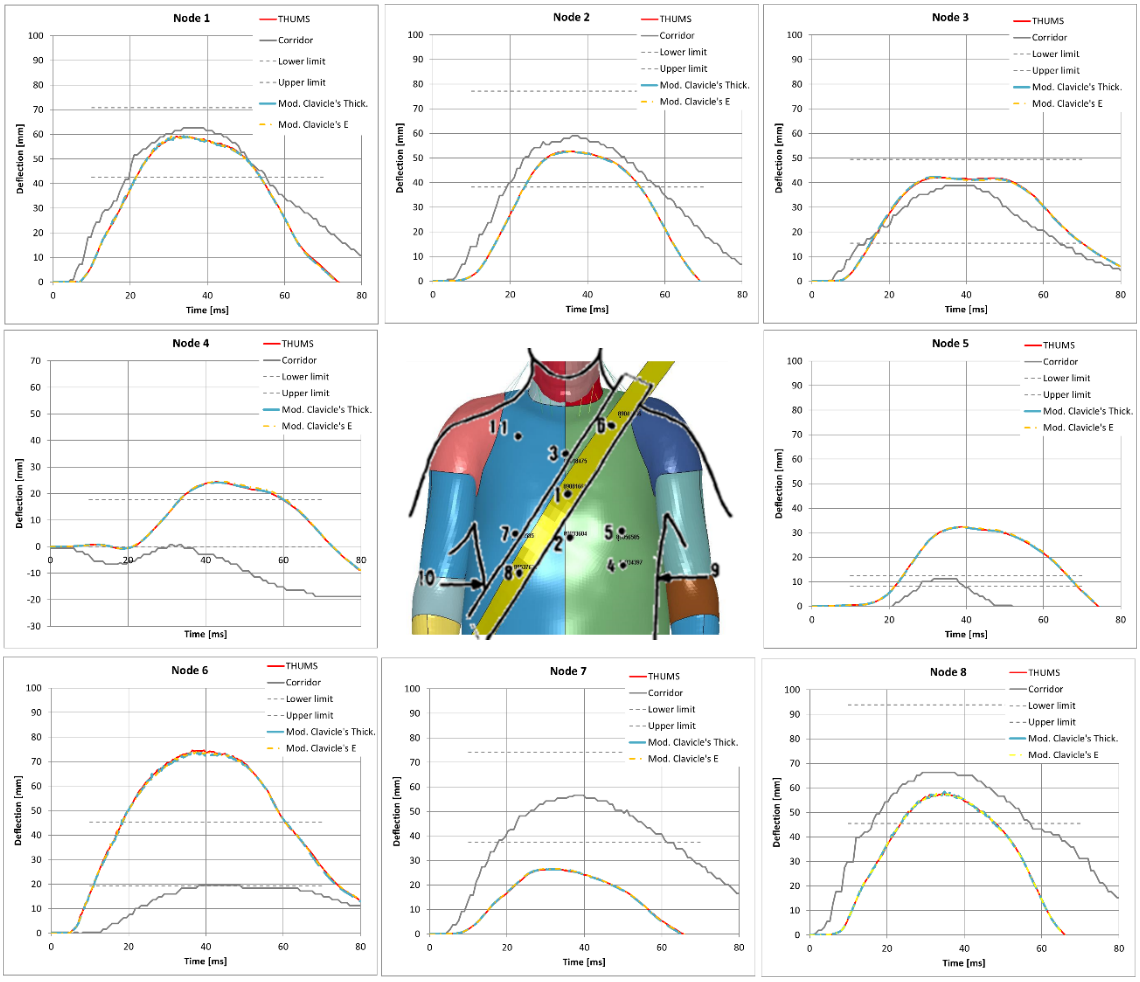

Figure 54 - Thorax - Belt validation impact for modified clavicles

Despite the changes do not have an effect on the stiffness problem, the model is more realistic and it can be seen from their impact on stress and strain. Figures 55-56 shows stress and strain maps, comparing the two simulations with the original one.

The shell thickness variation reduces the peak by 65% of the original value, indeed, in the middle, in which usually the force is applied, the tension results decreased. The same happens for the strain, indeed, where the thickness is higher than the original to support the load, especially in the middle, the strain values are smaller (Figure 56).

Young's modulus variation is more problematic than the previous case because, as mentioned before, the way to obtain the changes makes stress and strain distribution non-homogeneous. For both maps, there are different areas in which this effect can be seen. However, the trend is overall similar for the stress, the great difference can be seen for the strain, especially in the more elastic areas at the ends, for which the values are very high. This depends on the fact that, as in the real case, in those regions, the clavicle has to be deformable to allow the bone to support the load in the middle, indeed in the centre, the strain is smaller than the original case.

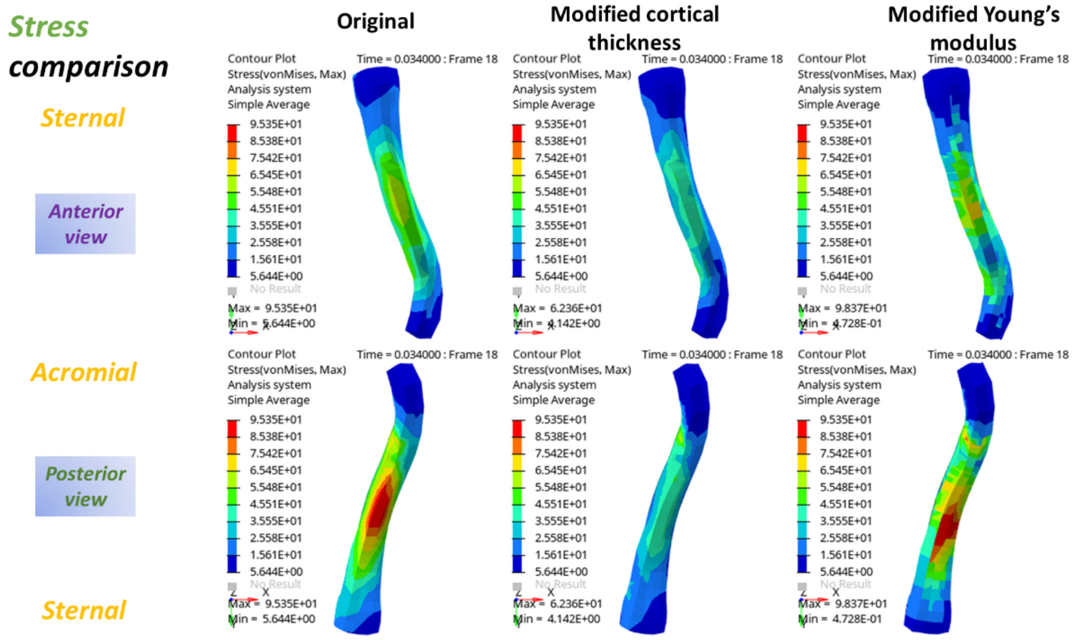

Figure 55 – Von Mises stress comparison

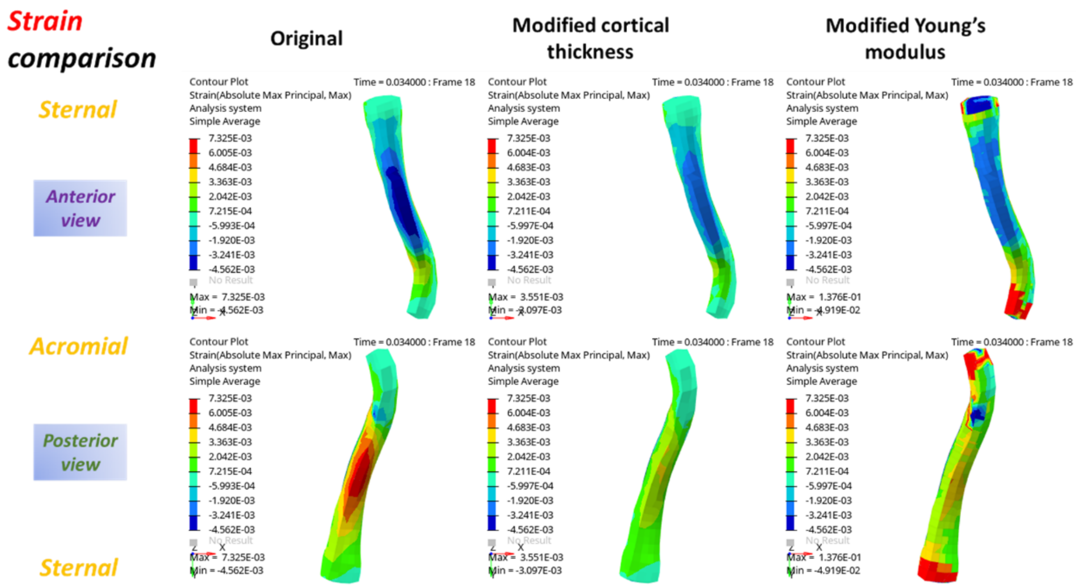

Figure 56 - Strain comparison

Therefore, the next step is to mesh again the shell with a thinner mesh to recreate a better Young's modulus distribution. Finally, the changes may put in a unique model and test it.

Displacement curves, for the unique model, will not probably change since the single modifications haven't had an effect on the response in the problematic impact. However, because these changes have an influence on stress and strain, making the condition more realistic than previous, they may nevertheless be maintained in the THUMS. It is now bio-faithful and later it may be validated for the rest of the impacts.

As regards ligaments properties, the limited literature available on their properties makes their characterization difficult. Two studies, in which tensile properties of the shoulder ligaments are investigated [34, 35], found different values of Young's modulus (E), density (ρ) and Poisson ratio (υ) (Table 1) compared to those set in the THUMS. While the two last parameters are closer to the ones of the model, Young's modulus is one order of magnitude smaller than the one set, and this value would change ligaments behaviour completely. Hence, since the difference between the values is too great, more studies should be considered before proceeding with the update.

***Table 1** - Material parameters for clavicle ligaments*

	Original parameters' model			**Gupta et al. 2011 [35]**		
	E [MPa]	ρ (t/mm^3)	υ	E [MPa]	ρ (t/mm^3)	υ
Acromioclavicular joint	140	$2 \cdot 10^{-9}$	0.4	10.6	$1 \cdot 10^{-9}$	0.3
Sternoclavicular joint	140	$2 \cdot 10^{-9}$	0.4	11.7	$1 \cdot 10^{-9}$	0.3
Coracoclavicular ligament	140	$2 \cdot 10^{-9}$	0.4	10	$1 \cdot 10^{-9}$	0.3

6.4 New spleen and liver introduction

Unlike the organs described above, the modification for the spleen and liver have been provided by Professor Bastien. The aim is to make the model more realistic and performances acceptable. The changes consist of new materials. Entire THUMS will be validated in this thesis using the same solver version used by Professor Bastien, 11.1 with single precision.

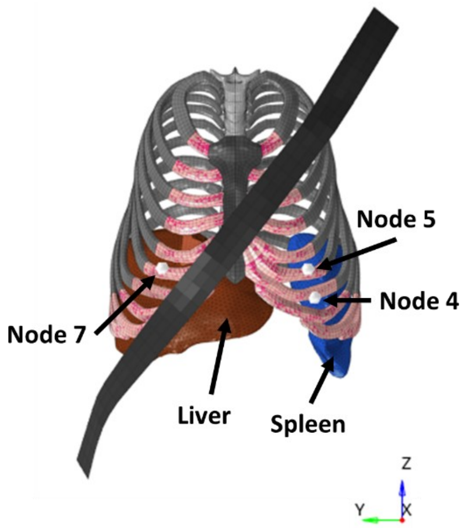

Figure 57 - Spleen and liver representation in THUMS with the belt and the problematic nodes

6.4.1 Liver

The introduced liver is characterized by a new material. In the original model, the liver was modelled with the material 181, MAT_SIMPLIFIED_RUBBER/FOAM, that is now replaced with material 57, MAT_LOW_DENSITY_FOAM.

Material 181 is a material used for solid elements defined by an engineering stress-strain curve that considers both compressive and tensile loads along one direction.

The new material 57 is indicated for the highly compressible parts. It is normally used for seat cushions and padding. Even in this case, there is the possibility to set a curve, indeed a nominal stress-strain's curve controls the liver's behaviour.

The last thing to do is to validate this new model. The old material is replaced with the new one in all THUMS impacts and the obtained results are compared with the original ones.

The models with new material for the liver almost follow original curves, which means that the new introduction has influenced neither force nor displacement results.

6.4.2 Spleen

Even a new material for the spleen is introduced. Like the liver, the spleen pass from the material 181 MAT_SIMPLIFIED_RUBBER/FOAM to the material 57 MAT_LOW_DENSITY_FOAM.

As always, the model must be validated, so impact simulations were run again. Unluckily, the Abdomen - Bar impact simulation did not work and for this reason, this chapter discusses all the attempts to understand the error and solve the problem.

The message file only returned the errors:

**** Error 40455 (SOL+455)*

NaN detected

**** Error 40456 (SOL+456)*

NaN detected.

reporting nodes and moments out of range. This is a general problem and to solve it you must understand what caused this fall out of range.

Energies plot is reported (Figure 58) comparing this model with the modified spleen and the original one presented in chapter 5. The curves are superimposed, this means that the simulation seems to work normally until the termination point, in which it falls in error.

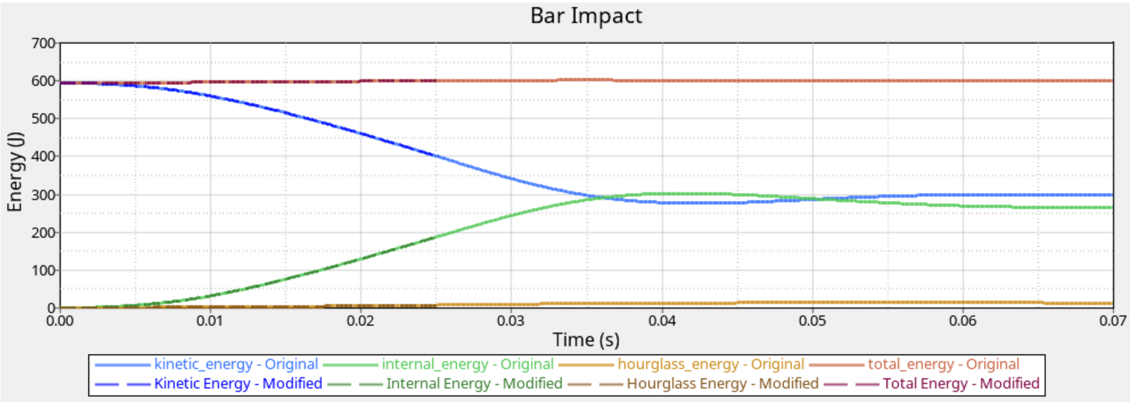

Figure 58 *- Energy comparison between THUMS with original and modified spleen*

Firstly, all message files are analyzed and some elements that seem to fail first are controlled. These elements are not focused on a single area but belong to different parts of the model even if are all located in the thoracic area.

The number of D3PLOT can be increased before the simulation fails, to see if something strange happens during the impact. DT is set to 0.5ms from 20ms to 27ms, keeping it unchanged elsewhere, but nothing out of normal behaviour is noticed.

Analysing the added mass for the original and modified models in figure 59, it is possible to notice two important spikes, with value graters than 50g. To better understand, in the graph are also reported the values for the two materials that normally has the major added mass, radio and ulna, that present values around 15-25g.

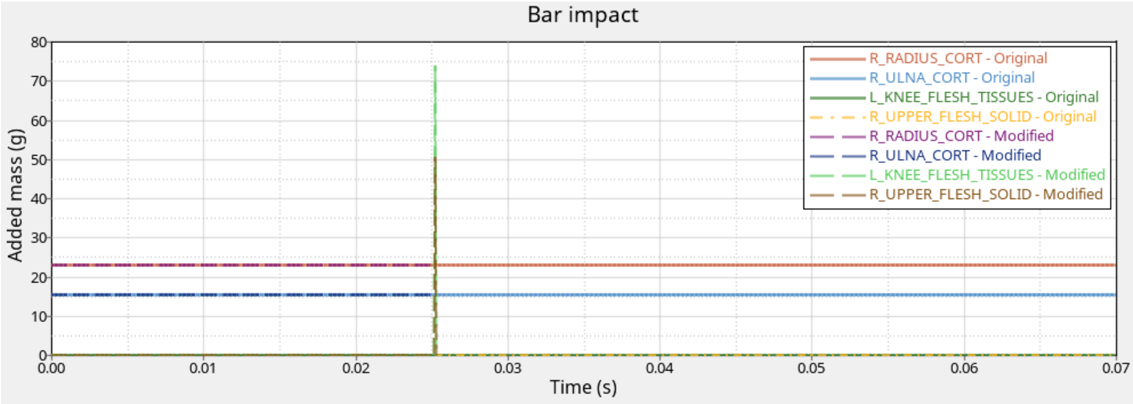

Figure 59 *- Added mass comparison between THUMS with original and modified spleen*

Added mass could be a great problem because represents not physical mass which actually does not exist. Time step size modification for mass scaled solutions (DT2MS) is tested to avoid a great increase.

As figure 60 shows, the spikes problem is solved by decreasing the DT2MS parameter by 10-20%. Also, some added mass presents in the original simulation disappear. Despite all, the simulation still does not work.

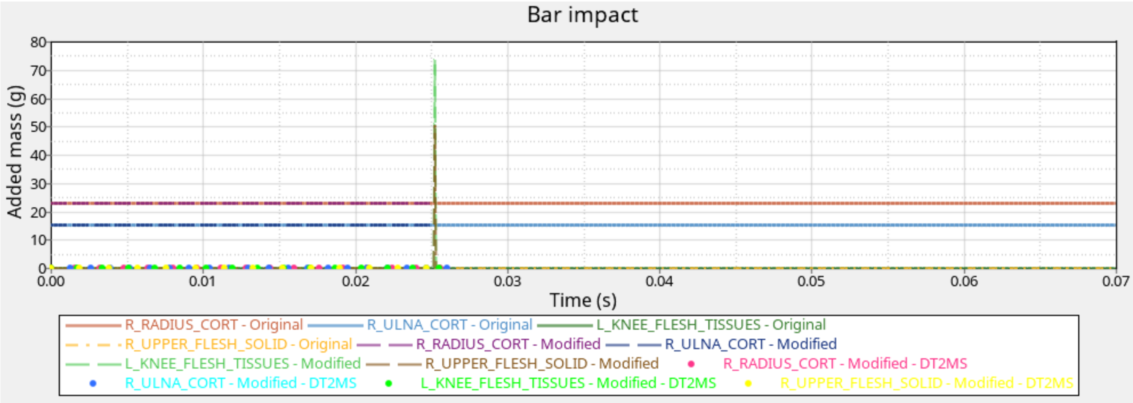

Figure 60 *- Comparison between THUMS with original and modified spleen and DT2MS modified simulation*

The next attempt is to try different solvers with which the simulation could work, combining different precision. Table 2 reports all types of solvers tested and relative outcomes; no one has been successful (Error termination).

Table 2 – Outcomes for simulations with different solvers and precision

Solver	*Precision*	Outcome
7	***Single***	Error termination
7	***Double***	Error termination
9	***Single***	Error termination
9	***Double***	Error termination
9.3	***Single***	Error termination
9.3	***Double***	Error termination
11	***Single***	Error termination
11	***Double***	Error termination
11.1	***Single***	Error termination
11.1	***Double***	Error termination

Another attempt to solve the problem is to focus on the section of the modified organ. Different formulations for tetrahedron elements are tried, even in combination with hourglass control modification (Table 3).

Remembering that spleen is one of the organs coated with a shell part, different element formulations (ELFORM) for the spleen coating's section are also used. As the table shows, no change solved the problem.

Table 3 - Outcomes for simulations with modified parameters

Spleen Section: ***Element formulation →***	***13 (original)***	***4***	***60***	***10***
Hourglass: 7 *(original)*	Error termination	Error termination	Error termination	Error termination
Hourglass: 4	Error termination	Error termination	Error termination	Error termination
Hourglass: 5	Error termination	Error termination	Error termination	Error termination
***Spleen coat section ELFORM: from* 4 *(original) to* 16**	Error termination	Error termination	Error termination	Error termination
***Spleen coat section ELFORM: from* 4 *(original) to* 27**	Error termination	Error termination	Error termination	Error termination

Lastly, it can be useful to mesh completely spleen coating and organ with a different average size of the elements. Professor Scattina has provided these parts. Results for the problematic impact, the abdomen bar impact, are shown in table 4. Original material is also tested to understand if the new mesh works as it should, and only the mesh with the average size of the elements did not work.

Table 4 -Outcomes for simulations with new spleen's mesh and different materials

Average size of spleen elements	***New material***	***Original material***
1mm	Error termination	Error termination
2mm	Error termination	Normal termination
3mm	Error termination	Normal termination

Energy for all simulations with modified material and organ meshed again is controlled, in comparison with the original simulation and the modified one (figure 61).

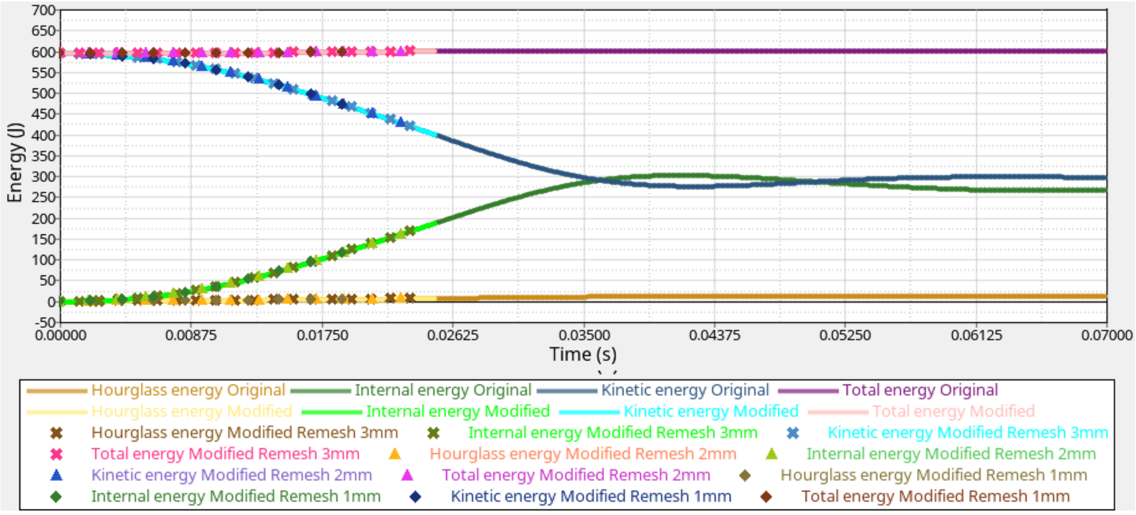

Figure 61 *- Energy comparison between THUMS with original and modified spleen and new spleen's mesh cases*

Every step tried until this point is repeated for these new models: different solvers and formulations. Unfortunately, no combination was successful, and another strategy is attempted.

Spleen coating material, in the original model, is modelled using material 34, MAT_FABRIC, usually used for the airbag and set to avoid excessive compressions. This type of material requires different parameters including the possibility to set two different Young's modulus, one for longitudinal direction and one for the transverse. This would lead to excessive rigidity on the model, for this reason, the material is changed from the 34th to material 9, MAT_NULL, to control contact with other parts without adding too much rigidity.

Abdomen – Bar impact simulation is run again with this change for all cases of the spleen with modified material and mesh and all fall in error as before (Table 5).

Table 5 *- Outcomes for simulations with modified material for the spleen and spleen coating*

Average size of spleen elements	*Simulation with MAT_NULL for spleen coating*
4mm (original size)	Error termination
3mm	Error termination
2mm	Error termination
1mm	Error termination

Once these paths have been attempted, it is taken a step back. The same models are run again with the original material for the spleen and the modified one for the coating, in order to understand if it were only the spleen's modified material the problem or not. The models work with the original material, except for the one with 1mm as size spleen elements, consistent with previous outcomes. The results are summarised and compared in table 6.

Table 6 - Outcomes for simulations with modified material for the spleen and spleen coating, using different average size of elements

Average size of spleen elements	*Simulation with original materials*	*Simulation with MAT_NULL for spleen coating*
4mm (original size)	Normal termination	Normal termination
3mm	Normal termination	Normal termination
2mm	Normal termination	Normal termination
1mm	Error termination	Error termination

Having regard to the outcomes, the new material for the spleen gets shelved, returning to the original one. However, a comparison of Von mises stress on the spleen can be useful to understand how the material of the spleen coating can influence the simulation (Figure 62). When null material is inserted, stress is greater than in the original simulation. On the contrary, the area affected by high stress is smaller as size decreases

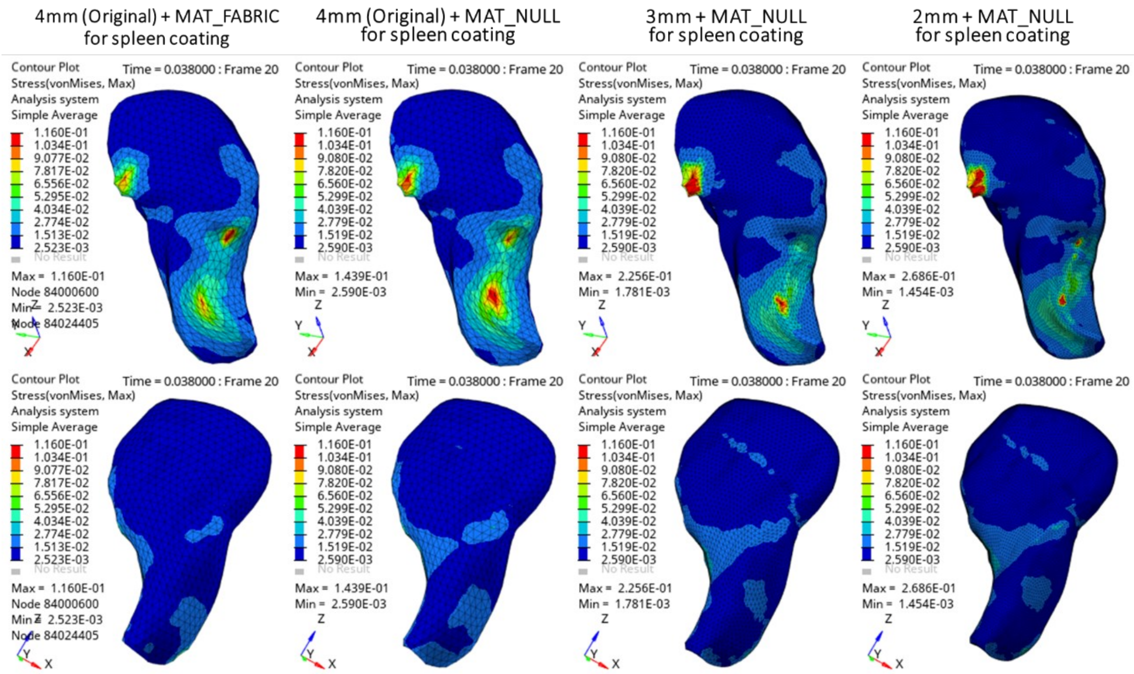

Figure 62 - Comparison for simulations with modified material for the spleen coating

The same comparison is carried out to see element size influence when original materials are set (Figure 63). As before, decreasing the dimension of the elements, major stresses localize in a small area concerning the original simulation (Size: 4mm). Moreover, as the size of the elements decreases, maximum Von Mises stress increase.

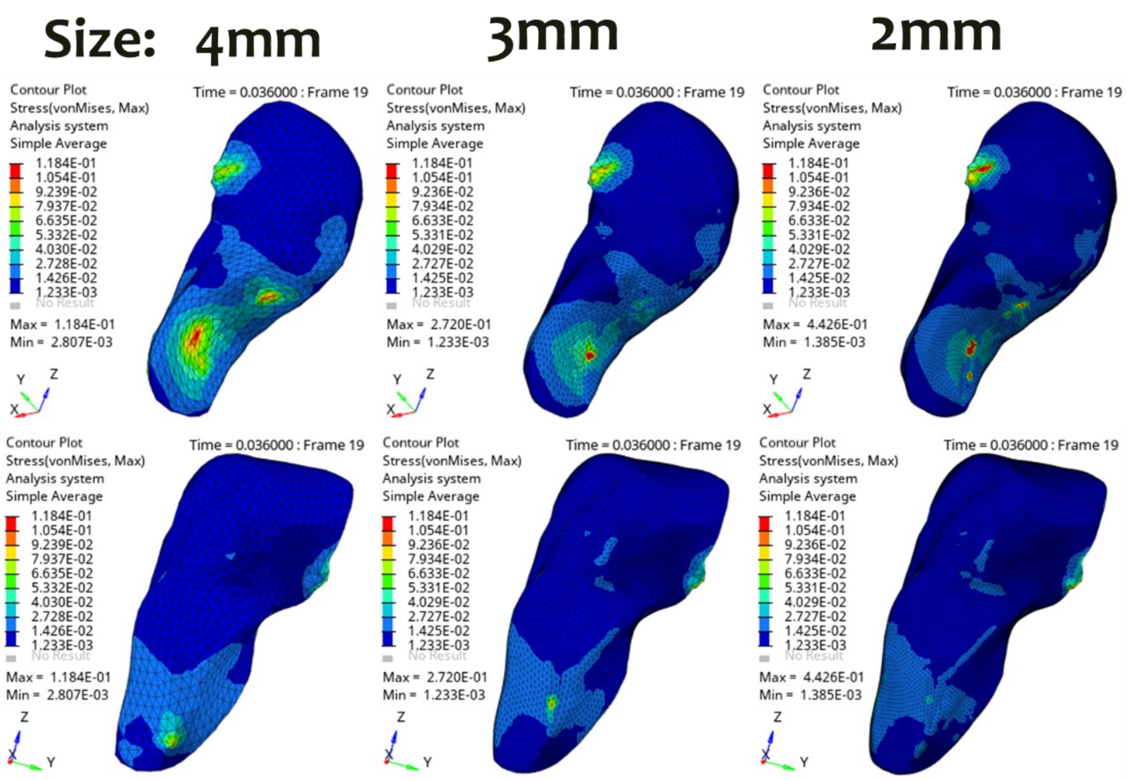

Figure 63 - Comparison of spleen with different average size of the elements

This comparison shows that also different mesh can influence biomechanical results and this different behaviour could have an effect on different impacts' simulations. Hence, different versions of THUMS, each with different spleen's mesh size, could be tested in the impacts of interest to figure out which is most bio-faithful.

Thesis Final Consideration

Nowadays, FEM models are increasingly used, indeed a wide application has been seen for the simulations of crash safety tests. However, it is important not only to have an accurate vehicle model but also for the occupants. THUMS is a human body computational model that has been developed to recreate its behaviour in detail. It also allows predicting injuries better than classic rigid dummies.

Nevertheless, it is not already a perfect tool, and for this reason, improvements are necessary. In this thesis work, made in collaboration with Professor Bastien of Coventry university, THUMS' properties have been investigated. The aim is to obtain a more bio-faithful model and the most risk impacts, presented in chapter 2, are recreated to verify the THUMS' behaviour, and validate it. For this reason, the main purpose is to make Thorax – Belt impact's curves of the problematic nodes fall into the right ranges. As shown in chapter 5, the right side of the body is too stiff, while the left side is too little rigid. Hence, different thoracic and abdomen organs, described in chapter 3, have been taken into account to try to obtain a more realistic behaviour:

- Costal cartilage is the first part of the body considered because the problematic curves are extracted from this component. A different model is attempted: the perichondrium is inserted going to surround the existing matrix. Unfortunately, no change has influenced the belt impact's response.

- The thoracic fat, below two of the problematic nodes, is then analyzed because of its large dimension. It was found that the organ may be rescaled to verify if this change can influence the thorax's stiffness.

- The clavicle is the third thoracic part which is considered because of its location under one of the nodes out of range. In particular, the clavicular cortical bone is better defined through a variable cortical thickness and Young's modulus distribution. However, displacement curves have remained unchanged, but these changes can be maintained in definitive THUMS, due to their great influence on stress and strain.

- Finally, new liver and spleen's materials are also introduced, from Professor Bastien's work. As in the other cases, new material for the liver did not have an effect on curves, while modified spleen material caused an error in simulations. Since no attempt solved the problem, the new material for the spleen is set aside, introducing instabilities.

Results allowed us to understand that small changes in a few parts of the body cannot influence too much model response in the impacts. Thickness and material changes are tested, but no one of them has been relevant in displacement curves. However, some had an effect on reducing the suffered stress or modifying strain conditions.

In the light of these considerations, the new THUMS with the modified clavicle and new liver's material could be imported in the sled model, briefly described in chapter 4. Finally, PVP's method should be applied to obtain AIS scores for the liver and spleen and compare them to those reported in the real-life accident.

Despite the few changes, THUMS is closer to reality than before and as written above, some of these analyses could be a good basis for future works. Other organs and parts of the body could be analyzed to continue with the improvements.

One final development of the work done is that only the model of the 50th percentile of the American male has been considered in this thesis, while there are different versions of THUMS, different from each other. They take into account the different sex and age groups, varying in properties and geometrical characteristics to better represents every single category. If then they are exposed to the same tests and are improved as is being done for the 50th percentile male model, it will be possible to use the appropriate model for each situation. The choice will, in all probability, influence a lot of biomechanical outcomes, including AIS score comparison, giving more accurate results.

Bibliography

[1] M. C. Toyota, “Total human model for safety (thums): revolutionizing crash simulation to support safe mobility for all,” 2021.

[2] T. Xu, X. Sheng, T. Zhang, H. Liu, X. Liang and a. A. Ding, “Development and Validation of Dummies and Human Models Used in Crash Test,” 2018.

[3] J. Zhao and G. Narwani, “DEVELOPMENT OF A HUMAN BODY FINITE ELEMENT MODEL FOR RESTRAINT SYSTEM R&D APPLICATIONS,” *TAKATA – Automotive Systems Laboratory, Inc.,* 2005.

[4] C. Kroell, S. DC and A. Nahum, “Impact tolerance and response of the human thorax,” *SAE International,* 1971.

[5] C. K. Kroell and D. C. Schneider, “Impact Tolerance and Response of the Human Thorax II,” *SAE International,* 1974.

[6] D. Cesari and Bouquet, R., “Behaviour of Human Surrogates Thorax under Belt Loading,” *SAE international,* 1990.

[7] Shaw, J.M., Herriott, R.G., McFadden, J.D., Donnelly, B.R., Bolte and J.H., “Oblique and lateral impact response of the PMHS thorax,” *50th Stapp Car Crash Journal.,* 2006.

[8] J. Cavanaugh, G. Nyquist and S. G. a. A. King, “Lower Abdominal Tolerance and Response”.

[9] W. Hardy, L.W.Schneider and S. Rouhana, “Abdominal Impact Response to Rigid-Bar,Seatbelt, and Airbag Loading”.

[10] J. D. Rupp, C. S. Miller, M. P. Reed, N. H. Madura, K. D. Klinich and L. W. Schneider, “Characterization of Knee-Thigh-Hip Response in Frontal Impacts Using Biomechanical Testing and Computational Simulations,” 2008.

[11] H. Guillemot, B. Besnault, S. Robin, J. LeCoz, F. Lavaste and J. Lassau, “Pelvic Injuries in Side Impact Collisions: A Field Accident Analysis and Dynamic Tests on Isolated Pelvic Bones,” *SAE Paper,* 1997.

[12] “Wikipedia,” [Online]. Available: https://en.wikipedia.org/wiki/.

[13] “TeachMeAnatomy,” [Online]. Available: https://teachmeanatomy.info/.

[14] J. L. Forman, E. d. P. d. Dios, C. A. Dalmases and R. W. Kent, “The Contribution of the Perichondrium,” *Journal of Biomechanical Engineering,* 2010.

[15] D. Dey, R. Nakazato, D. Li and D. S. Berman, “Epicardial and thoracic fat - Noninvasive measurement and clinical implications,” *Cardiovascular Diagnosis and Therapy,* 2012.

[16] W. G. Kwack, “Association between thoracic fat measured using computed tomography and lung function in a population without respiratory diseases,” *Journal of Thoracic Disease,* 2019.

[17] S. W. Rabkin, “Epicardial fat: properties, function and relationship,” 2006.

[18] J. Stojanovska, “Intrathoracic Fat Measurements Using Multidetector Computed Tomography (MDCT): Feasibility and Reproducibility,” 2017.

[19] Verhagen, “Local and systemic effects of visceral and perivascular adipose tissue,” 2012.

[20] J. Zhu, Z. Yang, X. Chen, J. Liu, L. Zheng, L. Zhang, J. Pi, G. Li, T. Zhuang, C. Liu, Y. Wang, L. Liu, L. Fan, P. Chan, B. Tomlinson, Y. Li, Z. Liu and Y. Zhang, “A Stronger Association of Epicardial Fat Volume with Non-Valvular Atrial Fibrillation Than Measures of General Obesity in Chinese Patients Undergoing Computed Tomography Coronary Angiography,” 2021.

[21] I. G., “Local and systemic effects of the multifaceted epicardial adipose tissue depot,” *Nat Rev Endocrinol,* 2015.

[22] S. Hyland, M. Charlick and M. Varacallo, “Anatomy, Shoulder and Upper Limb, Clavicle,” 2021.

[23] P. R. King, S. Scheepers and A. Ikram, “Anatomy of the clavicle and its medullary canal: a computed tomography study,” 2012.

[24] A. R. Kemper, J. D. Stitzel, C. McNally, H. C. Gabler and S. M. Duma, “Biomechanical Response of the Human Clavicle: The Effects of Loading Direction on Bending Properties,” *Journal of Applied Biomechanics,* 2009.

[25] X.-s. Qiu, X.-b. Wang, Y. Zhang, Y.-C. Zhu, X. Guo and a. Y.-x. Chen, “Anatomical Study of the Clavicles in a Chinese Population,” 2016.

[26] Z. Li, M. W. Kindig, J. R. Kerrigan and R. W. K. a. J. R. Crandall, “Development and validation of a subject-specific finite element model of a human clavicle,” 2011.

[27] “Association for the Advancement of Automotive Medicine,” [Online]. Available: https://www.aaam.org/abbreviated-injury-scale-ais/.

[28] C. Bastien, C. Neal-Sturgess, J. Christensen and L. Wen, “A Deterministic Method to Calculate the AIS Trauma Score from a Finite Element Organ Trauma Model (OTM),” 2019.

[29] G. Mondino, “Human Body Model and Passive Safety of Vehicles: Analysis of biomechanical results and study of injuries on abdomen organs,” 2021.

[30] J. L. Forman and R. W. Kent, “The effect of calcification on the structural mechanics of the costal cartilage,” 2012.

[31] J. L. Forman and R. W. Kent, “Modeling costal cartilage using local material properties with consideration,” *Journal ofBiomechanics,* 2011.

[32] J. ANDERMAHR, A. JUBEL, A. ELSNER, J. JOHANN, A. PROKOP, K. E. REHM and J. KOEBKE2, “Anatomy of the Clavicle and the Intramedullary Nailing of Midclavicular Fractures,” 2007.

[33] R. E. Chen, S. P. Soin, R. El-Shaar, G. T. Nicandri, H. A. Awad, M. D. Maloney and I. Voloshin, “What Regions of the Distal Clavicle Have the Greatest Bone Mineral Density and Cortical Thickness? A Cadaveric Study,” 2019.

[34] S.-W. Koh, J. M. Cavanaugh and J. P. Leach, “MECHANICAL PROPERTIES OF THE SHOULDER LIGAMENTS UNDER QUASI-STATIC AND DYNAMIC LOADING,” *Ircobi Conference,* 2004.

[35] A. K. Gupta, G. Sharma, P. Shah, C. Ageorges and C. Mayer, “Development of an anatomically-correct finite element model of the human shoulder,” *Ircobi Conference,* 2011.

Acknowledgements

A conclusione di questo elaborato, vorrei ringraziare tutti coloro che ne hanno permesso la realizzazione.

In primis, desidero ringraziare il mio relatore Alessandro Scattina per la sua disponibilità e tempestività nel seguire il mio lavoro, dandomi la possibilità di accrescere le mie competenze.

Un doveroso *"Thank you"* va al mio correlatore, il professor Christophe Bastien, per le conoscenze trasmesse con pazienza e costanza.

Un ringraziamento speciale va alla mia collega Giulia Mondino per aver condiviso con me questa lunga esperienza.

Infine, voglio dedicare questo mio traguardo a tutta la mia famiglia, che nonostante le mie paure mi ha sempre supportata.

Grazie.